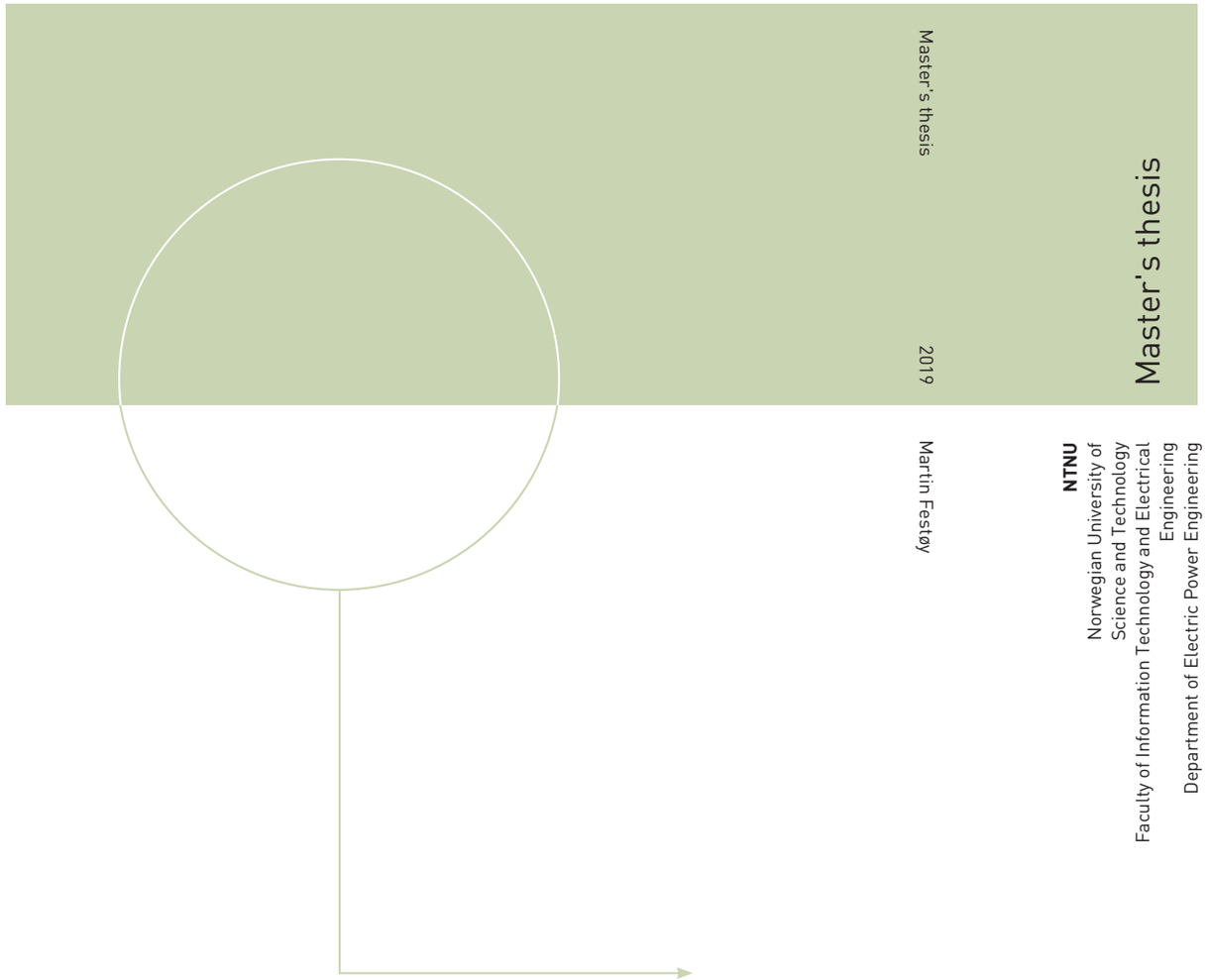

Master's thesis

2019

Martin Festøy

NTNU
Norwegian University of
Science and Technology
Faculty of Information Technology and Electrical
Engineering
Department of Electric Power Engineering

Martin Festøy

Voltage Control for Distribution Systems using Chance Constrained Linear AC OPF

June 2019

NTNU
Norwegian University of
Science and Technology

NTNU
Norwegian University of
Science and Technology

NTNU
Norwegian University of
Science and Technology

Voltage Control for Distribution Systems using Chance Constrained Linear AC OPF

Martin Festøy

Energy and Environmental Engineering
Submission date: June 2019
Supervisor: Hossein Farahmand
Co-supervisor: Jamshid Aghaei

Norwegian University of Science and Technology
Department of Electric Power Engineering

Preface

This document is a master's thesis written at the *Department of Electric Power Engineering* within the *Norwegian University of Science and Technology (NTNU)*. The thesis has been written during the spring of 2019, and is the conclusion of a five year master's degree within Energy and Environmental Engineering.

This thesis is a continuation of the project *Distributed Voltage Control in Smart Distribution systems*, which was written during the fall of 2018. This thesis is however to be considered as an independent publication, and thus some parts of the project have been rewritten. As a consequence, there are some similarities in sections 1.5, 1.6 and 1.7

The reader is presented with most of the basic theory required to understand the thesis, and thus only fundamental knowledge about electrical power and statistics is required to read this document.

12-06-2019

Acknowledgments

I would like to thank my supervisor, associate professor Hossein Farahmand. Although he has a very busy schedule, he always provided useful insight when I came asking. I would also like to extend my most sincere gratitude to postdoc. Venkatachalam Lakshmanan for helping me complete my model, and providing valuable insight writing the thesis.

A special thank you is aimed at PhD candidate Naser Hashemipour at the university of Shiraz, Iran. His help in interpreting the model was irreplacable, and without him this thesis would not have been possible.

I would also like to thank all of my friends at Studentersamfundet i Trondhjem. Because of you, these last five years have been some of the best years of my life, and for that I am forever grateful.

Martin Hergot Festøy

June 2019

Abstract

The global energy market is rapidly evolving. Ever-rising demand for distributed renewable energy, as well as changing habits of consumption require new ways to regulate voltage to enable maximum renewable penetration in the power system, and at the same time ensure security of supply. To that end, this thesis will present an optimization model that combines the voltage regulating efforts of tap changers and distributed photovoltaic (PV) inverters to improve the voltage profile of the distribution system.

At the same time, a key challenge of solar PV is the uncertain, intermittent behavior. To account for the uncertainty in both generation and demand, a chance constrained framework will be implemented in the optimization model. The chance constrained framework will help quantify the uncertainty of the problem without depending on any historical data from the system. In fact, the method only relies on a forecast and a maximum forecast error.

The optimization model is implemented on the IEEE 33-bus distribution test system, and then tested for multiple variations of the system, including: No distributed renewables, 1 MW PV at bus 30, different size variations of the PV and inverter, introduction of energy storage, and lastly decentralizing PV and storage to multiple buses. Additionally, the forecast error is adjusted, and the impact on the constraints of the optimization is presented.

The conclusion of the different optimization scenarios showed a clear improvement in overall voltage profile at all buses when the distributed PV was installed. Furthermore there was some improvement in the voltage for increased inverter size, increased PV capacity, and for the introduction of energy storage. The results showed a significant improvement in overall bus voltage when the PV and storage were decentralized.

The constraints of the optimization problem were shown to tighten with a higher relative forecast error, and consequently, a better voltage profile means that the solution to the optimization problem is viable for higher forecast errors. Thus, the cost of upgrading the distributed system can be seen as the cost of certainty.

Sammendrag

Det globale energimarkedet er i rask utvikling. Den stadig økende etterspørselen etter distribuert fornybar energi, samt endring av forbruksvaner, krever nye måter å regulere spenning for å muliggjøre maksimal fornybar penetrasjon i kraftsystemet, samtidig som forsyningssikkerheten bevares. Av den grunn vil denne avhandlingen presentere en optimaliseringsmodell som kombinerer den spenningsregulerende kapasiteten til distribusjonstransformatorer og vekselrettere tilkoblet distribuerte solceller, for å forbedre spenningsprofilen til distribusjonssystemet.

Samtidig er en stor utfordring med solceller den usikre, intermittente oppførelsen. For å ta hensyn til usikkerheten i både generering og etterspørsel, vil et sannsynlighets-avgrenset rammeverk bli implementert i optimaliseringsmodellen. Dette gir mulighet til å kvantifisere usikkerheten, uten å avhenge av historiske data fra systemet. Faktisk er metoden bare avhengig av en prognose og en maksimal prognosefeil.

Optimaliseringsmodellen er implementert i IEEE sitt 33-buss testsystem, og testet for flere variasjoner av systemet, inkludert: Ingen distribuert fornybar energi, 1 MW solceller ved buss 30, forskjellige størrelsesvarianter av solceller og vekselretter, innføring av energilagring og til slutt desentraliserte solceller og energilagring til flere busser. I tillegg blir prognosefeilen justert, og effekten på optimaliseringsproblemets begrensninger presenteres.

Resultatene fra de ulike optimaliseringsscenariene viste en klar forbedring i total spenningsprofil på alle busser da distribuert PV ble installert. Videre var det noen forbedringer i spenningen for økt størrelse på vekselretter, økt størrelse på solceller og for innføring av energilagring. Resultatene viste en signifikant forbedring i busspenning når solceller og energilagring ble desentralisert.

Begrensningene til optimaliseringsproblemet ble strengere for høyere relativ prognosefeil, og følgelig betyr en bedre spenningsprofil at optimaliseringsproblemet har en potensiell løsning for høyere prognosefeil. Dermed kan kostnadene ved å oppgradere distribusjonssystemet betraktes som kostnaden for sikkerhet.

Contents

List of Figures

List of Tables

Abbreviations

PV	Photovoltaic
IEEE	Institute of Electrical and Electronics Engineers
OLTC	On load tap changer
EV	Electric vehicle
CCO	Chance constrained optimization
OPF	Optimal power flow
PDF	Probability distribution function
CDF	Cumulative distribution function
P.U	Per Unit
MPPT	Maximum power point tracking
MILP	Mixed integer linear programming
SOC	State of charge
STATCOM	Static synchronous compensator

1 Introduction

This chapter will start by outlining the problem description and motivation behind the thesis, as well as the specific contribution of this thesis and the scope. The general structure of the thesis is then presented, followed by the relevant background theory that is required to understand the thesis.

1.1 Problem description & motivation

Currently, distribution networks are experiencing a significant share of photovoltaic (PV) integration. The PV systems can provide reactive power control as vital means to provide voltage support. However, widespread use of local reactive power control by PV systems can interfere with existing voltage regulation schemes by the distribution system operators. To enable a higher penetration of renewables in the distribution system, it is therefore necessary to address this challenge.

At the same time the generation from PV is at all times subject to the irradiation, and this can be hard to forecast precisely. Thus a model that deals with generation from PV should also consider the uncertainty involved when simulating the system. PV generation is also purely limited to the time of day the sun shines. To better utilize and further enable high PV penetration distribution grids, some form of energy storage is highly desirable.

1.2 Contribution

In this thesis, a coordinated operation of distributed voltage controllers/reactive power compensators is modeled that reveals an appropriate operation that brings the performance of the tap-changer and distributed generation sources together.

The suggested method will take into account the impact of the forecast error of power demand and PV generation, and thus adopt the chance constrained framework to consider uncertainty without requiring the historical data of the system.

For testing the method, a linearized optimization problem will be implemented on the standard

Institute of Electrical and Electronics Engineers (IEEE) 33-bus network. After the initial simulation, basic sensitivity analysis will be performed on the system, with specific focus on how changes to the system impacts the voltage profile and chance constraints.

1.3 Scope

To narrow down the scope of this massive problem, this thesis will do a couple of simplifications, as well as some general assumptions:

- Most importantly, the system will be linearized to increase computational efficiency. As such, this thesis will also be an example of the viability of a linearized AC power flow model.
- The tap changer as well as the energy storage will be modeled as "black-boxes" with somewhat simplified equations describing them
- The model will not consider constraints on line flow
- The optimization is done with 1 hour time increments. Thus the behavior of the system is assumed stationary during each hour.
- The relative forecast error of load and generation will be assumed equal
- Economic profitability is primarily overlooked. Instead the thesis focuses on technical limitations.

The implications of these points will be thoroughly discussed in chapter 4

1.4 Structure

The remainder of chapter 1 will provide the required theoretical insight into general distribution level voltage generation and scheduling, as well as background on chance constrained modeling and linear optimization. Therefore, only a basic understanding of electrical power and statistics is necessary prior to reading this thesis.

Chapter 2, *Method*, will in depth explain the mathematical formulation of the model, and the details about how it is implemented as an optimization problem.

Chapter 3, *Results and analysis*, will present and explain the results from the implementation of the basic model, as well as all relevant results gained from the sensitivity analysis.

Chapter 4, *Discussion*, will first discuss the implications of the results at length, before discussing the validity and strengths / weaknesses of the model.

Chapter 5, *Conclusion and further work*, will draw conclusions from the discussion presented in chapter 4, and provide suggestions for further improvements on the work.

1.5 Theoretical background

1.5.1 Current energy situation

The global energy market is changing towards more renewable sources, and an increasing amount of these renewables are distributed renewables. That is: renewable energy sources connected directly to the distribution grid. One such renewable source is photovoltaics(PV), showing an increase in worldwide installed capacity from about 1.2 GW in year 2000, to approximately 303 GW by the end of 2016. China alone installed 34.5 GW in 2016, and consequently became the country with the highest cumulative installed capacity at 78 GW [3].

As a whole, PV technology has several advantageous properties. It is renewable, practically maintenance free, and completely silent. It is also well suited for installation on areas that would otherwise be unused, like rooftops. The two latter properties are what makes PV ideal for distributed installation. PV technology has also rapidly fallen in price in recent years. 2016 marked a milestone in PV price development, as large PV investments became cheaper than on-shore wind power [4]

Distributed PV offers a lot of promising possibilities to the system. Most prominently, placing the generation close to the consumer may decrease the total transmission losses. Additionally there may be less severe voltage drops on heavy load in weak distribution grids. Due to the low maintenance and nonexistent need for fuel, PV generation has a marginal cost of practically zero. That means that when first installed, there is no added cost to producing full power over leaving the system idle. This is in stark contrast to most dispatchable generation types like coal or gas. These types of generation often have a cost attributed to both starting and increasing generation, as well as much higher maintenance costs.

However, there are several difficulties with large-scale implementation of distributed renewables. Several of these difficulties are consequences of the unreliable output of PV modules, as rapid changes in generation may lead to both over-voltages as well as faster degradation of traditional voltage regulation devices like on load tap changers(OLTCs). Additionally, if more power is produced than consumed at the distribution level, power might start flowing in the wrong direction. This is a fundamentally challenging problem, since the traditional power system is explicitly designed for unidirectional power flow.

While wind power may have its generation decrease due to low wind speed at night and in the

early morning, solar PV is unique in its clear discrepancy between when the bulk of the power is generated, and when the load is at its peak. This phenomena has been labeled the “duck curve”, due to the graph of the net load looking somewhat like a duck[1]. Counteracting the duck curve is one of the most pressing challenges in networks with high PV-penetration.

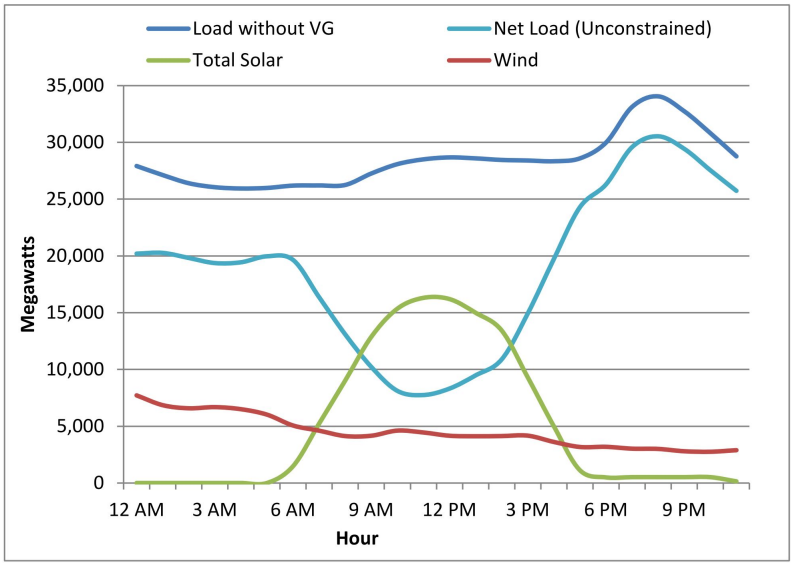

Figure 1: An example of the duck curve on a spring day in California. *Figure from [1]*.

An uncomplicated method to avoid over-voltages from intermittent PV-generation, is to curtail excess generation. Generation curtailment, in the broad sense of the word, is to use less power than is potentially available at a given time. However, the world as a whole wants to cut emissions, so curtailment of a cheap renewable energy source is generally undesirable.

While curtailment may sometimes be necessary to avoid back-feeding of power into the OLTC, the owners of the curtailed energy are not always reimbursed for the loss of income, and thus frequent curtailment could decrease overall incentive to invest in non-dispatchable renewables like PV [5],[6]. Additionally, curtailment of excess energy does not address the “duck curve” problem. The obvious solution is the introduction of some type of energy storage.

1.5.2 Energy storage systems

For most of power system history there has been widespread agreement that electric energy cannot be stored in large quantities. This fact is, however, becoming gradually less true, as progress in storage systems has increased in recent years. Energy storage is often presented as the only solution

to widespread installation of non-dispatchable renewables like solar and wind. Both as a way of providing ancillary services, and as a way of counteracting the “duck curve" [7].

Several different technologies are now becoming available for storing electrical energy. In terms of total stored energy, pumped hydro storage is by far the most widespread technology, accounting for over 95% of global storage capacity[8]. For obvious reasons, however, pumped hydro storage is unsuited for distribution level storage.

One increasingly used option is grid connected batteries, which has seen a rise in recent years. Currently electro-chemical storage (i.e batteries) represents some 2% of the total worldwide storage capacity and almost 62% of active storage projects[8]. Additionally, battery technology has skyrocketed in recent years, driven partly by the fast increasing popularity of electric vehicles (EVs) and consumer electronics.

Among the electro-chemical storage technologies, the Lithium-ion battery has become one of the most researched and commonly used. This is mainly because the Lithium-ion batteries have a relatively high specific energy and specific power, which makes them particularly suitable when used in portable storage like electric vehicles and small electronics. An overview of specific power and energy for some storage solutions can be seen in figure 2. While the specific energy and power is less important for stationary appliances, the fast development of Lithium-ion batteries may benefit the industry as a whole.

One drawback of most types of electro-chemical storage, is that it degrades over time. While battery degradation is less dramatic in stationary appliances than in mobile ones like EVs, the batteries will still have to be replaced from time to time. As with most energy conversion processes, electrochemical storage also has losses involved. The relatively cheap lead-acid battery can typically have an efficiency of 85%, while the significantly more expensive lithium-ion batteries may have significantly higher efficiencies [2].

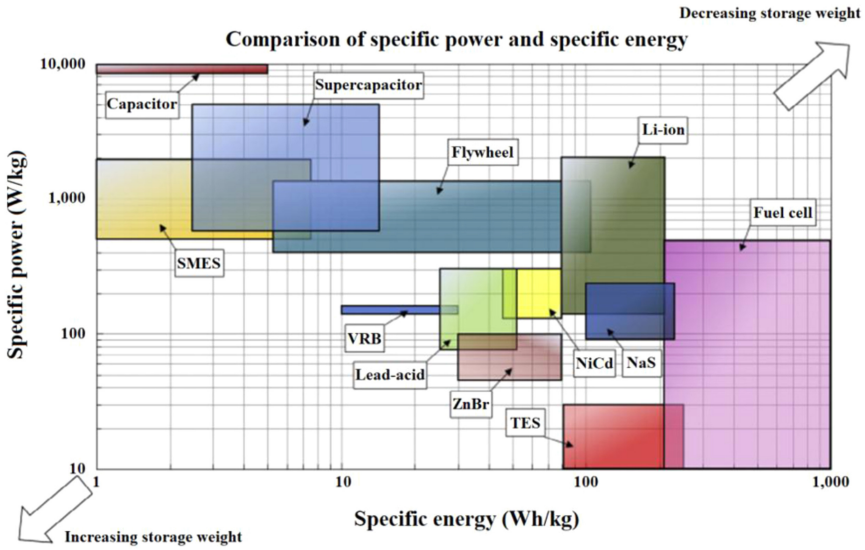

Figure 2: Specific power and energy of some storage solutions. *Figure from [2]*.

1.5.3 Reactive power control

Another solution to voltage fluctuations from intermittent PV generation, is to use the inverters connected to each PV panel to provide reactive power control. Reactive power control is already the preferred way to control voltage in the transmission network, but in the distribution network it is less so. In the transmission system, power flow between adjacent buses is often simplified as:

$$P_s = \frac{V_s \cdot V_r}{X} \cdot \sin(\delta_s - \delta_r) \tag{1.1}$$

$$Q_s = \frac{V_s^2}{X} - \frac{V_s \cdot V_r}{X} \cdot \cos(\delta_s - \delta_r) \tag{1.2}$$

Where subscripts s and r represent sending and receiving end values respectively. Additionally, P and Q is the Active and reactive power flow respectively, V and δ is the voltage magnitude and angle at the bus respectively, and X is the reactance of the connecting line. Thus it is clear to see that there is a strong relation between reactive power and voltage when $\delta_s - \delta_r \approx 0$. However resistance values are negated in these equations, due to $X >> R$ in the transmission network.

In the distribution system, however, the $\frac{R}{X}$ ratio is significantly higher than in the transmission system. The result is that while still feasible, reactive power control will lead to much higher real losses when used for voltage regulation. Another common issue is the difficulty of installing and maintaining switched capacitors in the distribution system.

The latter is one of the reasons why it is favorable using the inverters for reactive power control, as they are already a necessity for installing solar power. Additionally, most installations will not produce power at full capacity all the time due to insufficient irradiation. That means that the inverters don't necessarily need to be oversized to be able to contribute to voltage regulation.

Local reactive power control based on inverters used in distributed generation has been thoroughly researched in the last 15 years, and numerous scientific articles have been released on the subject. Among these are [9],[10],[11],[12],[13] and many others. A general conclusion is that while there is a stronger relation between active power and voltage in the distribution system, reactive power support from distributed inverters has still proven to be an effective way of stabilizing voltages. In particular, inverters are useful in dealing with the local over-voltages that often accompany distributed PV-generation.

1.6 Chance constrained optimization

Chance constrained optimization (CCO) is a technique used to apply uncertainty to optimization problems. As mentioned in [14], the key uncertain parameters involved in distributed voltage regulation are all possible to forecast. PV output is forecastable by weather forecasting, and load profiles rarely change dramatically from expected values. In fact the day ahead scheduling of the power market is entirely based on the load being somewhat predictable.

As a consequence, the uncertain variables in them self are not necessary to model. Instead it is possible to simply account for how the variables may vary from the forecasted value. In other words: The forecasting error. If X is the actual value of the variable, X_0 is the forecasted value, and ΔX is the forecasting error, then:

$$X = X_0 + \Delta X \tag{1.3}$$

CCO applies this error to the modeling of the system by adding probabilistic constraints to the equations. CCO is a quite robust method, however, it is often difficult to solve as it depends heavily on probability distribution functions (PDF), which are often difficult to formulate[15]. This is especially true for nonlinear cases, of which AC optimal power flow (OPF) is an example. A significant advantage of using CCO is that if the error in the forecasts can be modeled, then there is no need for historical data from the system to apply uncertainty.

There are numerous recent examples of literature that use CCO for uncertainty modeling in power systems. *M. Hajian et al.*[16] use CCO for an online voltage control system with an uncertain amount of load available for load-shedding. Articles [17],[18],[19],[20] all use CCO for optimal resource utilization in transmission systems, while [21] use CCO for energy storage planning in distribution systems.

When it comes to applying CCO, *H. Bludszuweit et al.*[22] mention that the kurtosis of the weather forecasting error PDF typically has values ranging from 3 to 10, where 3 is normal for day ahead forecasting, and 10 or greater is very short term forecasting. Continuing, it is stated that the forecasting error PDF has a close to symmetrical behavior. As 3 is the kurtosis of a univariate normal distribution, the normal distribution function can be applied when modeling the forecasting error for day ahead forecasts.

A key feature of the normal distribution function is that the expected value is zero. Thus the average error of the problem will also be zero, making the problem easier to implement. This is especially useful when linearizing nonlinear AC power-flow, which will be mentioned further in section 1.7.

To implement the normally distributed variables, the cumulative distribution function (CDF) can be utilized. More specifically the quantile function, K, which is the inverse of the CDF. Intuitively that means that if the CDF represents a function $F(x)$ that returns the probability of X being smaller than or equal to some value x as shown in (1.4), then the quantile gives the x that would make $F(x)$ return a specific value. In equation form:

$$\Pr(X \leq x) = F(x) \tag{1.4}$$

$$F^{-1}(\alpha) = \mathrm{K}(\alpha) = x \tag{1.5}$$

For the purpose of this paper, α represents the level of uncertainty tolerance, and has a known value that can be decided on a simulation basis. The quantile function will return a value when given an uncertainty tolerance α. However to return the correct value, the normal distribution of which the quantile is derived will have to be scaled appropriately. As mentioned, the normal distribution will have a mean value of 0 and a kurtosis of 3. Thus the scaling will be solely subject to the standard deviation of the distribution, which will have to be calculated for all the individual uncertain parameters.

From the properties of the normal distribution, it is known that 99.9% of all the possible errors are placed within the interval $\pm 3\sigma$, where σ is the standard deviation. Thus if $err_{\max}$ is the upper limit of forecasting error for a specific forecasting procedure, then the standard deviation, σ can be calculated as:

$$\sigma = \frac{err_{\max}}{3} \tag{1.6}$$

If we then apply a known parameter, ε as the relative value of the forecasting error with respect to the forecasted value:

$$\varepsilon = \frac{err_{\max}}{X_0} \tag{1.7}$$

Then standard deviation can be written as:

$$\sigma = \frac{\varepsilon X_0}{3} \tag{1.8}$$

Thus, equation (1.8) can be used to calculate the standard deviation of a forecasted variable, X_0, if the relative forecasting error has been determined.

1.7 Linear AC power-flow

AC optimal power-flow is in it self a nonlinear problem, and as a consequence, optimization problems done on any moderately sized system will be very computationally demanding. Additionally adding chance constraints will not make the problem more computationally efficient, so other solutions have to be examined in order to get practical computation times over multiple iterations.

In the precursor project for this thesis, it was concluded that linear programming is a highly advantageous solution method when applicable. This is mainly because of the vastly superior computation speeds compared to the nonlinear alternative, as well as being relatively easy to implement[23].

The main drawback of linear programming is loss of accuracy. This is not an issue for inherently linear problems, but presents itself as a problem when linearizing nonlinear systems. Thus linear programming is only a feasible option when the system is already linear, or when the nonlinear system can be linearized without significant loss of accuracy.

Linearization of AC power flow is not to be confused with the frequently used DC power flow. DC power flow, although linear, is a result of simplifications and assumptions about voltage magnitude and resistance in the transmission system. It is well suited for fast system calculations, but results are often infeasible in real systems [24].

Application of the DC-OPF model in distribution systems would suffer from these infeasibilities at an even worse scale, due to the the inherent properties of the distribution grid. In particular the higher R upon X ratio, since DC power flow is based on neglecting resistance altogether.

Multiple articles have shown the feasibility of linearizing AC power flow. In [25], *A. Garces* provide a framework for linear load flow for three-phase distribution systems. Despite the linearization, the method is quite accurate compared to the commonly used back-forward sweep algorithm. Articles [24], [26] and [27] show linearized AC power flow utilized for somewhat different purposes. Thus the solutions are not identical, however, they all show the feasibility of a solution. Additionally, [26] demonstrates a solution for a distributed case, and as such is highly relevant. Lastly, [10] presents a set of linearized equations for the PV inverter. Variations of these equation will be shown in chapter 2.

2 Methodology

In this chapter, the methodology of the thesis will be described. Section 2.1.1 will present the basic mathematical outline of the problem, while sections 2.1.2 - 2.1.9 will present the specific equations required to implement this model. Lastly, section 2.2 will present how the model is implemented for computer modeling.

2.1 Mathematical formulation

This section will present the mathematical formulation of the optimization problem. Most equations have been derived from fundamental power system analysis or statistics, while some have been derived from a paper by *Jamshid Aghaei* and *Naser Hashemipour* that is currently under review. However, a conference paper describing the basis for the article can be found at [28].

2.1.1 Basic problem outline

The basis of any optimization problem is to find out what to optimize, and formulate the objective function. In this case, the objective is to minimize voltage difference of the buses relative to 1 per unit (P.U), where 1 P.U is the given base voltage of the system.

This objective function will be subject to several constraints. In this case, the constraints are the maximum and minimum allowed voltage values, the load flow of the system and the inverter rating. Additionally, it is desirable that the PV unit delivers as much active power to the grid as the solar irradiation allows. In other words, active power injection from PV should follow the PV MPPT-curve, that is: the maximum power point tracker of the PV system. Thus, the basis for the optimization problem can be described as equations (2.1) - (2.5):

$$\min \sum_{i,t} |V_i(t) - 1| \tag{2.1}$$

$$h(X) = 0 \tag{2.2}$$

$$V_{\min} \leq V_i(t) \leq V_{\max} \tag{2.3}$$

$$P_g^2(t) + Q_g^2(t) \leq S_{inv}^2 \tag{2.4}$$

$$P_{g_i}(t) = P_{MPPT_i}(t) \tag{2.5}$$

Here (2.1) is the objective function which is to minimize voltage, V, deviation from 1 P.U for all buses, i over all time steps, t. Equation (2.2) represents the power flow equations which will be described in detail in section 2.1.5, and equation (2.3) is the voltage upper and lower limits at each bus. Lastly (2.4) describes the capacity curve of the PV inverter, and (2.5) ensures that maximum active power is delivered from the PV unit. The inverter capacity curve is a curve that limits the active and reactive power output of the inverter, P_g and Q_g respectively, so that the total apparent power does not exceed the inverter limit, S_{inv}.

Note that equations (2.1) - (2.5) are the basic equations describing the optimization problem, but some will have to be transformed to be applicable in a chance constrained linear model. This will be shown in the remaining part of this chapter.

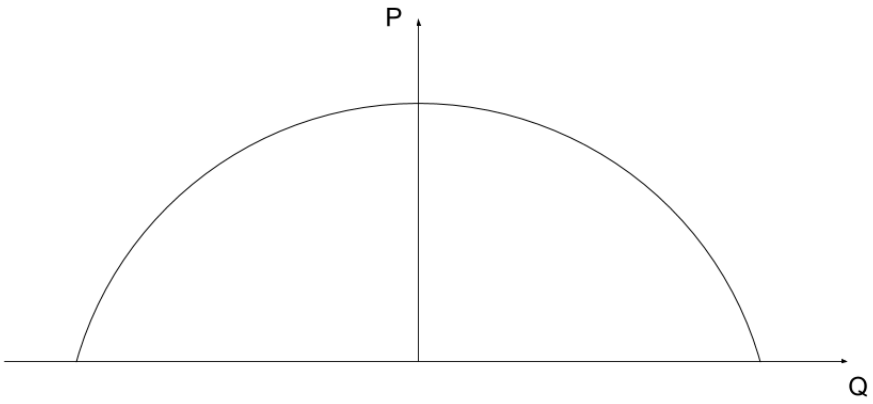

Figure 3: The inverter capacity curve in the P-Q plane.

2.1.2 Basic chance constrained implementation

The modeling of the uncertainty has been divided into three steps. First the upper bound of the day ahead forecasting error of PV and demand is determined, $\varepsilon_{\max}$. The upper bound of the forecasting error is then used to calculate the standard deviation of the forecasting error, which ultimately is used to solve the chance constrained optimal power flow.

As mentioned in section 1.6, CCO is based on writing uncertainty as probabilistic constraints. For some arbitrary uncertain parameter $\tilde{\beta}$ with PDF f and CDF F, there are two methods of implementing chance constraints:

Method 1:

$$\tilde{\beta} \leq g_1(X) \tag{2.6}$$

$$\Pr\left(\tilde{\beta} \leq g_1(X)\right) \geq 1 - \alpha \tag{2.7}$$

Here g is some arbitrary function of X, and $\Pr$ represents probability. By the definition of the PDF and CDF, (2.7) can then be written as:

$$\Pr\left(\tilde{\beta} \leq g_1(X)\right) = f\left(\tilde{\beta} \leq g_1(X)\right) \geq 1 - \alpha \tag{2.8}$$

Consequently, the chance constraint is implemented as:

$$f\left(\tilde{\beta} \leq g_1(X)\right) = F\left(g_1(X)\right) \geq 1 - \alpha \tag{2.9}$$

Since the CDF is an ascending function, (2.9) can be written using the quantile $\mathrm{K}(x)$:

$$g_1(X) \geq \mathrm{K}(1 - \alpha) \tag{2.10}$$

Method 2:

$$g_2(X) \leq \tilde{\beta} \tag{2.11}$$

$$\Pr\left(g_2(X) \leq \tilde{\beta}\right) \geq 1 - \alpha \tag{2.12}$$

And then similarly as in method 1, the relation between PDF and CDF gives:

$$\Pr\left(g_2(X) \geq \tilde{\beta}\right) = f\left(g_2(X) \geq \tilde{\beta}\right) \tag{2.13}$$

$$f\left(g_2(X) \geq \tilde{\beta}\right) = 1 - F\left(g_2(X) \geq \tilde{\beta}\right) \geq 1 - \alpha \tag{2.14}$$

$$F\left(g_2(X) \geq \tilde{\beta}\right) \leq \alpha \tag{2.15}$$

$$g_2(X) \leq \mathrm{K}(\alpha) \tag{2.16}$$

For both methods, α represents the level of uncertainty tolerance in the model.

2.1.3 Calculating the quantile function

As mentioned in section 1.6, to implement the quantile functions shown in methods 1& 2, the standard deviation of the uncertain parameters will have to be calculated. The uncertain parameters in this case is the load and generation of each bus. For the buses without generation, only the load is uncertain. The standard deviation of real and reactive power at those buses can thus be found by utilizing equation (1.8):

$$\sigma_{P_i} = \frac{\varepsilon P_{l_i}}{3} \tag{2.17}$$

$$\sigma_{Q_i} = \frac{\varepsilon Q_{l_i}}{3} \tag{2.18}$$

In buses with PV generation, the active power generation is another uncertain variable. For two normally distributed parameters with mean μ and standard deviation σ, the following properties apply:

$$\begin{aligned} a &\sim \mathcal{N}(\mu_a, \sigma_a) \\ b &\sim \mathcal{N}(\mu_b, \sigma_b) \\ a \pm b &\sim \mathcal{N}\left(\mu_a \pm \mu_b, \sqrt{\sigma_a^2 + \sigma_b^2}\right) \end{aligned} \tag{2.19}$$

Thus the standard deviation for the net power at a PV bus is calculated as:

$$\sigma_{P_{ni}} = \frac{\varepsilon\sqrt{P_{g_i}^2 + P_{l_i}^2}}{3} \tag{2.20}$$

To simplify the implementation of the CCO, the error in power and reactive power can be transferred to the voltage variable as a constraint. Since the forecast error is relatively small, the relation between power and voltage can be written as:

$$\begin{bmatrix} \boldsymbol{\Delta P} \\ \boldsymbol{\Delta Q} \end{bmatrix} = Jac \times \begin{bmatrix} \boldsymbol{\Delta \delta} \\ \boldsymbol{\Delta V} \end{bmatrix} \tag{2.21}$$

Here Δ is the difference between the forecasted and actual value, and Jac is the Jacobian matrix of the system used in power flow analysis. The Jacobian matrix is inversed to calculate the voltage from the real and reactive power, and the inverse of the Jacobian is divided into four sub-matrixes like:

$$(Jac)^{-1} = \begin{bmatrix} J_1^{-1} & J_2^{-1} \\ J_3^{-1} & J_4^{-1} \end{bmatrix} \tag{2.22}$$

So that:

$$\boldsymbol{\Delta V} = J_3^{-1} \times \boldsymbol{\Delta P} + J_4^{-1} \times \boldsymbol{\Delta Q} \tag{2.23}$$

Thus applying the relation (2.19), the standard deviation of the voltage error can be calculated as:

$$\sigma_{v_i} = \sqrt{\sum_j \left(\left(J_3^{-1}(i,j)\sigma_p(j) \right)^2 + \left(J_4^{-1}(i,j)\sigma_q(j) \right)^2 \right)} \tag{2.24}$$

As a result the uncertainty related to real and reactive power can be transferred to the voltage constraints, as will be shown in equations (2.43)-(2.44)

2.1.4 Inverter capacity

As mentioned, the inverter capacity curve is presented in equation (2.4). Plotting this constraint in the P-Q plane results in a semi-circle like the one presented in figure 3. To convert (2.4) to a chance constrained inequality, the following methodology is used:

If $\tilde{P}_g$ is the actual value of active power generation at the bus, P_{g0} is the forecasted value of generation and $\Delta\tilde{P}_g$ is the forecasting error, then the relationship between these can be written as:

$$\tilde{P}_g = P_{g0} + \Delta\tilde{P}_g \tag{2.25}$$

The inverter capacity must be upheld, thus the original capacity curve (2.4) can be rewritten as:

$$\tilde{P}_g = \sqrt{S_{inv}^2 - Q_g^2} \tag{2.26}$$

Inserting (2.25) into (2.26):

$$\Delta\tilde{P}_g \leq \sqrt{S_{inv}^2 - Q_g^2} - P_{g0} \tag{2.27}$$

Now utilizing the method for implementing chance constraints shown in section 2.1.2 on inequality (2.27), the inverter capacity curve ends up as:

$$\left(P_{g_{inv}} + \mathrm{K}(1-\alpha) \right)^2 + Q_{g_{inv}}^2 \leq S_{inv}^2 \tag{2.28}$$

In practice, the constraint added from $\mathrm{K}(1-\alpha)$ means that the area of the capacity curve is smaller than before adding the chance constraints. This difference is illustrated in figure 4. Additionally it can be seen that higher forecasting error leads to a more constrained capacity curve. When there is no solar generation the inverter capacity is simple to model, as the inverter will be fully dedicated to provide reactive power support. Thus the inequality constraints for the no generation hours are:

$$Q_g \leq S_{inv} \tag{2.29}$$

$$Q_g \geq -S_{inv} \tag{2.30}$$

However, when there is solar generation the inverter will focus on delivering active power foremost, and then supply reactive power by capacity. To implement these constraints in a linear model,

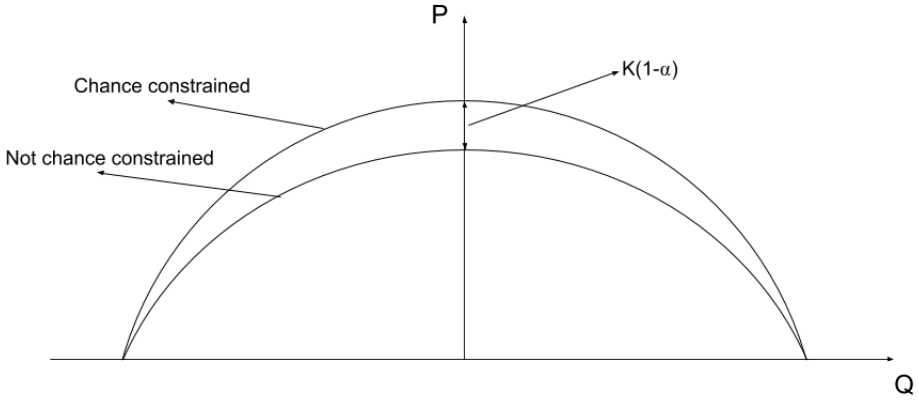

Figure 4: Visualization of the impact of the chance constraints on the inverter capacity curve.

the inverter capability curve will have to be linearized. The linear solution space for the supplied reactive power can be found by utilizing the maximum potential reactive output (2.31), and the minimum power factor (2.32):

$$Q_{\max} = \sqrt{S_{inv}^2 - P_g^2} \tag{2.31}$$

$$\cos\phi = \frac{P_g}{S_{inv}} \tag{2.32}$$

Where P_g is the active power delivered by the inverter for a specific hour. Thus the capability curve may be linearized as equations:

$$P_g - \left(\frac{S_{inv} - P_g(-Q_{\max})}{Q_{\max}}\right) \cdot Q_g \leq S_{inv} \tag{2.33}$$

$$P_g - \left(\frac{S_{inv} - P_g(Q_{\max})}{-Q_{\max}}\right) \cdot Q_g \leq S_{inv} \tag{2.34}$$

$$Q_g \leq S_{inv}\cos\phi \tag{2.35}$$

$$Q_g \geq -S_{inv}\cos\phi \tag{2.36}$$

However, since equations (2.33)&(2.34) contain uncertain elements, they will have to be chance constrained. Using methods shown in section 2.1.2, equations (2.33)&(2.34) can be written in chance constrained version as equations (2.37)&(2.38):

$$P_g - \left(\frac{S_{inv} - P_g(-Q_{\max})}{Q_{\max}}\right) \cdot Q_g \leq S_{inv} - \mathrm{K}(1-\alpha) \tag{2.37}$$

$$P_g + \left(\frac{S_{inv} - P_g(Q_{\max})}{-Q_{\max}} \right) \cdot Q_g \leq S_{inv} - \mathrm{K}(1-\alpha) \tag{2.38}$$

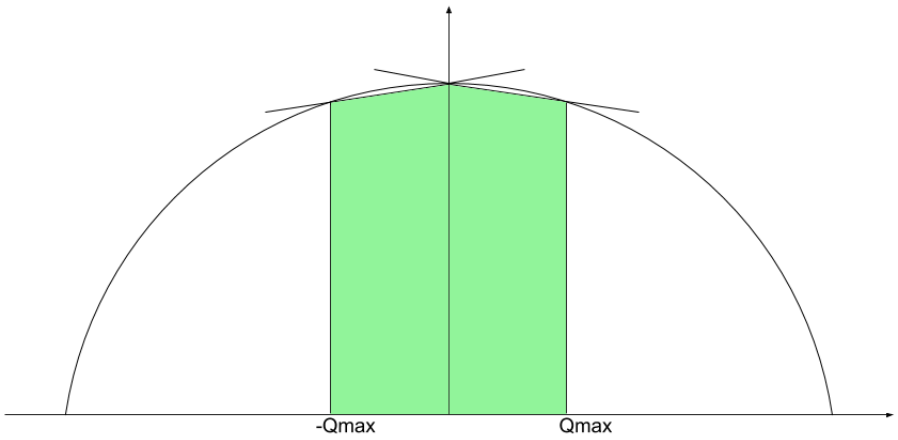

Figure 5: The linearized inverter capacity curve.

2.1.5 Power flow

Equations (2.39) - (2.40) represent the traditional power flow equations.

$$P_{n_i} = P_{g_i} - P_{l_i} = \sum_j V_i V_j Y_{ij} \cos(\delta_i - \delta_j - \theta_{ij}) \tag{2.39}$$

$$Q_{n_i} = Q_{g_i} - Q_{l_i} = \sum_j V_i V_j Y_{ij} \sin(\delta_i - \delta_j - \theta_{ij}) \tag{2.40}$$

Where P_{n_i} and Q_{n_i} represent net active power at bus i and net reactive power at bus i respectively. Subscripts g_i and l_i represent generation and load at bus i respectively. Y_{ij} and θ_{ij} represent the magnitude in p.u and angle of the admittance of the connecting branch. As previously, V_i is the voltage magnitude at bus i, and δ_i, δ_j represent the voltage angle at buses i and j respectively.

To be able to apply linear programming, equations (2.39) - (2.40) will have to be linearized. Since the magnitudes and angles of the voltages will have values around 1 and 0 respectively, the standard load flow equations will be linearized around these points [25]:

$$P_{n_i} = \sum_j Y_{ij} [\cos\theta_{ij} + \cos\theta_{ij} \cdot (V_i - 1) + \cos\theta_{ij} \cdot (V_j - 1) - \sin\theta_{ij} \cdot \delta_j + \sin\theta_{ij} \cdot \delta_i] \tag{2.41}$$

$$Q_{n_i} = \sum_j Y_{ij}[\cos\theta_{ij} \cdot \delta_i - \sin\theta_{ij} \cdot (V_i + V_j - 1) + \cos\theta_{ij} \cdot \delta_j] \tag{2.42}$$

2.1.6 Voltage limits

As shown in equation (2.3), the voltage of the buses is to be kept within a specified range. To implement chance constraints into equation (2.3), methods 1&2 from section 2.1.2 can be applied. Thus the upper limit of the voltage is applied as:

$$V_i \leq V_{\max} - \mathrm{K}(1-\alpha) \tag{2.43}$$

And the lower limit is applied as:

$$V_i \geq V_{\min} + \mathrm{K}(\alpha) \tag{2.44}$$

2.1.7 The objective function

To be able to apply linear programming, the non-linear objective function shown in equation (2.1) has to be linearized. Since an absolute value is not a linear equation, the objective can be reformulated as:

$$\min \sum_{i,t} y_{i,t} \tag{2.45}$$

Subject to constraints:

$$y_{i,t} \geq V_{i,y} - 1,\ y_{i,t} \geq 1 - V_{i,t},\ y_{i,t} \geq 0 \tag{2.46}$$

Thus the objective is defined by only linear equations.

2.1.8 Modeling the tap changer

In a distribution system where insufficient PV to cover all demand is installed, it is also necessary to model the tap changer at the slack bus. Since tap changers are based on changing transformer taps between several distinct positions, the voltage at the slack bus is not a strictly continuous variable. Instead it is a discrete variable that can only take on a specified number of values. This changes the whole problem from a linear programming problem to a Mixed integer linear programming (MILP) problem. The impact of this change will be discussed further in section 3.1.1.

2.1.9 Implementing energy storage

As mentioned in section 1.5, some form of energy storage is highly desirable when implementing large scale distributed PV generation to avoid curtailment. A simple, technology-independant en-

ergy storage model can be implemented based on the model presented in [29]. The storage is placed on the DC side of the PV inverter, and is only charged directly from the PV panels. Additionally, this model is easy to implement in every single PV bus in the system.

For a given PV bus at time step t, active power delivered to the inverter, $P_g(t)$ can be written as:

$$P_g(t) = P_{PV}(t) + P_B(t) \cdot \eta \tag{2.47}$$

Where $P_{PV}(t)$ is generated power from PV, $P_B(t)$ is battery power, and η is the round trip efficiency of the storage. Note that $P_B(t)$ can be both positive and negative for discharging and charging respectively.

The amount of energy stored at a given time, $E_B(t)$ can be written as:

$$E_B(t) = E_B(t-1) - P_B(t) \tag{2.48}$$

Equations (2.47)-(2.48) are then subject to the following constraints:

$$0 \leq E_B(t) \leq E_{B\,\max} \tag{2.49}$$

$$-P_{B\,\min} \leq P_B(t) \leq P_{B\,\max} \tag{2.50}$$

$$P_B(t = \text{night}) \geq 0 \tag{2.51}$$

Where equations (2.49)-(2.50) keep the variables within the given component limits, and (2.51) tell the system that the batteries should never charge using grid power, only PV. Additionally it may be desirable that the storage start each day not depleted, but rather with a specific state of charge, SOC_{start}. This can be ensured using the following constraints:

$$\begin{aligned} E_B(t = \text{startofday}) &= SOC_{\text{start}} \cdot E_{B\,\max} \\ E_B(t = \text{endofday}) &= SOC_{\text{start}} \cdot E_{B\,\max} \end{aligned} \tag{2.52}$$

2.2 Implementation

The suggested approach has been modeled on the standard IEEE 33-bus system with a 1 MW PV unit connected to bus 30. The inverter of the PV unit has been somewhat oversized to 1.054 MVA to enable effective reactive power control. The system has a base voltage of 12.66 kV, and the voltage limits were set to $V_{\max} = 1.05\,\text{P.U}$ and $V_{\min} = 0.95\,\text{P.U}$. The optimization was done over 24 hours, and in 1 hour increments. The load and PV irradiation profiles can be seen in figure 7, and the data for the load and PV profiles can be found in appendix A.

For the scenario with energy storage, a generic storage with round trip efficiency of $\eta = 0.9$ was implemented at the PV bus. An efficiency of 0.9 is roughly equivalent of a really good lead-acid battery, but worse than the best li-ion batteries. The storage had a maximum power of $P_{B\,\max} = 5\,\mathrm{MW}$, state of charge at start $SOC_{\mathrm{start}} = 0.4$, and $E_{B\,\max} = 15\,\mathrm{MWh}$.

The optimization was done using the *Pyomo* language [30] for Python 3.6, and using the *GUROBI* solver. The opimization was run on a laptop computer with a Intel(R) CORE m 1.40 GHz CPU and 8GB of RAM. The figures have been generated using the package *matplotlib* for Python.

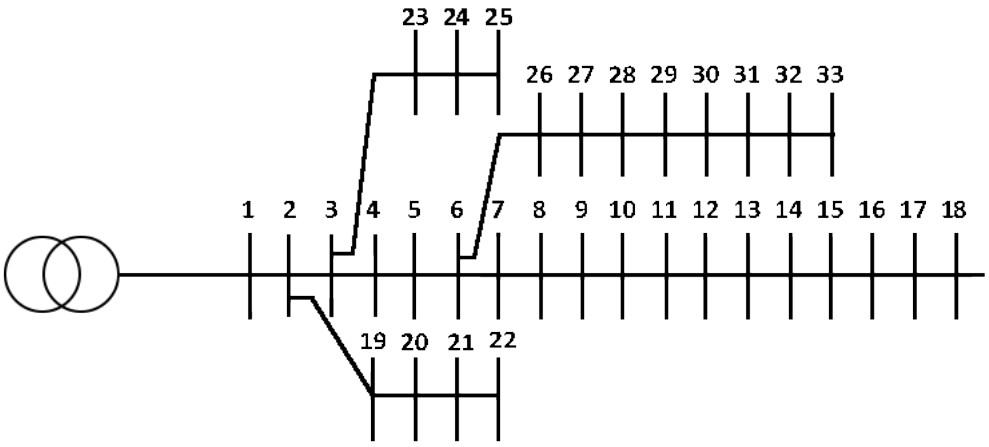

Figure 6: The IEEE 33-bus distribution system.

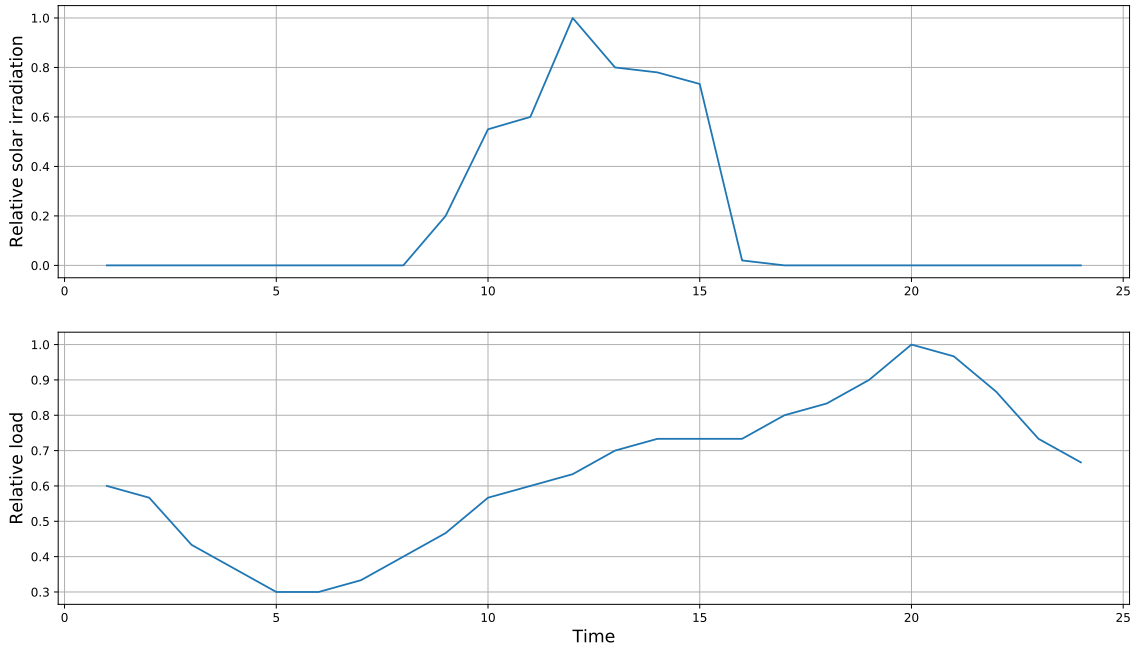

Figure 7: The 24 hour irradiation and load data used.

3 Results and analysis

This chapter will focus primarily on presenting the optimization results for the model. First the base case without energy storage will be presented. With the base case, the impact of a simplified tap changer model will be presented, as well as the impact of changing the relative forecast error. Then the impact of increasing the installed PV will be studied in section 3.1.4, and the impact of increasing the inverter size in section 3.1.5.

In section 3.2, a generic energy storage system is added to the PV bus, and the effects are studied. The PV system is then expanded considering storage in section 3.2.1. In section 3.3, the distributed PV is decentralized, and the effects are observed. Lastly an equivalent system without distributed PV is optimized to better understand the difference between the scenarios in section 3.4.

3.1 Base case without storage

In the base case the system described in section 2.2 was simulated over a 24 hour period, using the load and irradiation data provided. The level of uncertainty tolerance was set to $\alpha = 0.1$ and the relative value of the forecasting error is set to $\varepsilon = 0.1$

It can be seen in figure 8 that both positive and negative voltage deviation from 1 P.U is significantly larger in the peak load hour (hour 20) than in the peak PV hour (hour 12). This is partly because the load is significantly lower at peak PV hour, but also because the extra generation from the PV helps with supplying the rest of the grid. As a consequence, the voltage at the slack bus does not need to be as high at peak PV hour.

It can be noted that the sudden change in voltage from bus 18 to 19 is due to different radials. As can be seen in figure 6, bus 18 is at the end of the main radial while bus 19 is connected to bus 2. Thus the total line impedance to bus 18 will be higher, and consequently the voltage loss is higher.

Studying figures 9 and 10, the impact of the PV system can be seen. Most notable is the expected drop in power delivered from upstream grid in the PV production hours, as well as the inverter covering a very large part of the reactive power demand outside of PV production hours.

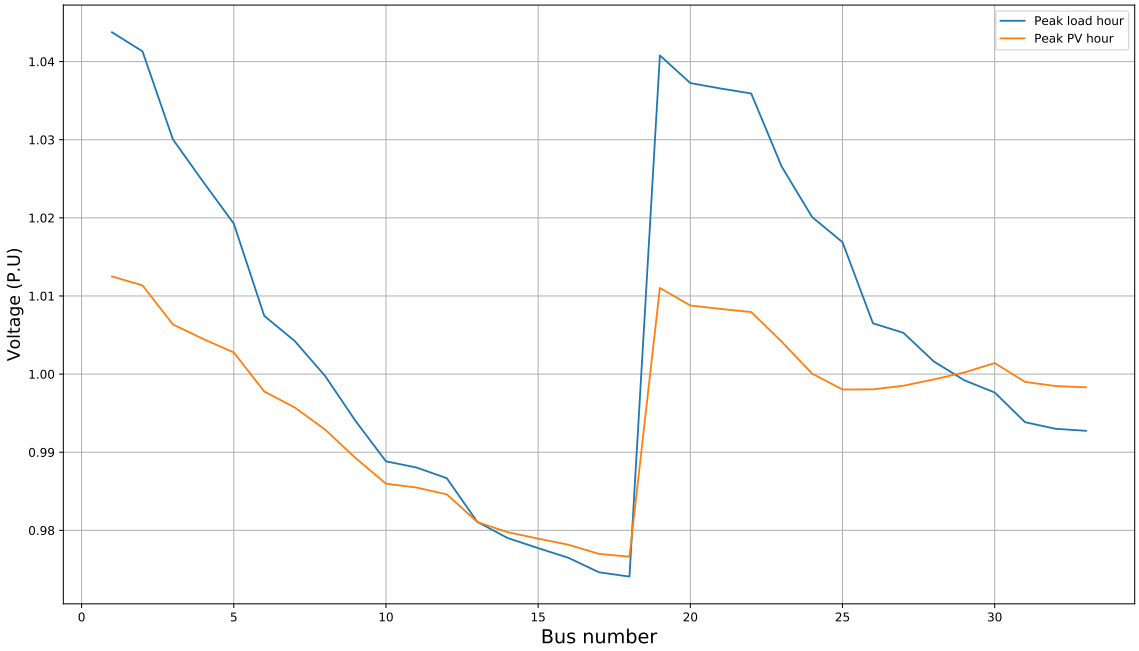

Figure 8: The bus voltage seen at peak load hour and peak PV-production hour, base case.

Figure 11 shows a plot of the acceptable voltage range for each bus at peak load hour. Also represented in the plot is the actual voltage at each bus for this time. Since the maximum and minimum voltage values are predecided scalars, the deviation in the lines from exactly 1.05 and 0.95 can be attributed to the chance constraints. It can be noted that the chance constraints change the voltage limits based on the consequence of a wrong forecast. Subsequently the constraints are more narrow around bus 24-25, due to those buses having significantly larger load demand than the rest. Bus 30 also has more narrow constraints, due to the PV system placed at the bus. The impact of changing the forecasting error will be further studied in section 3.1.3.

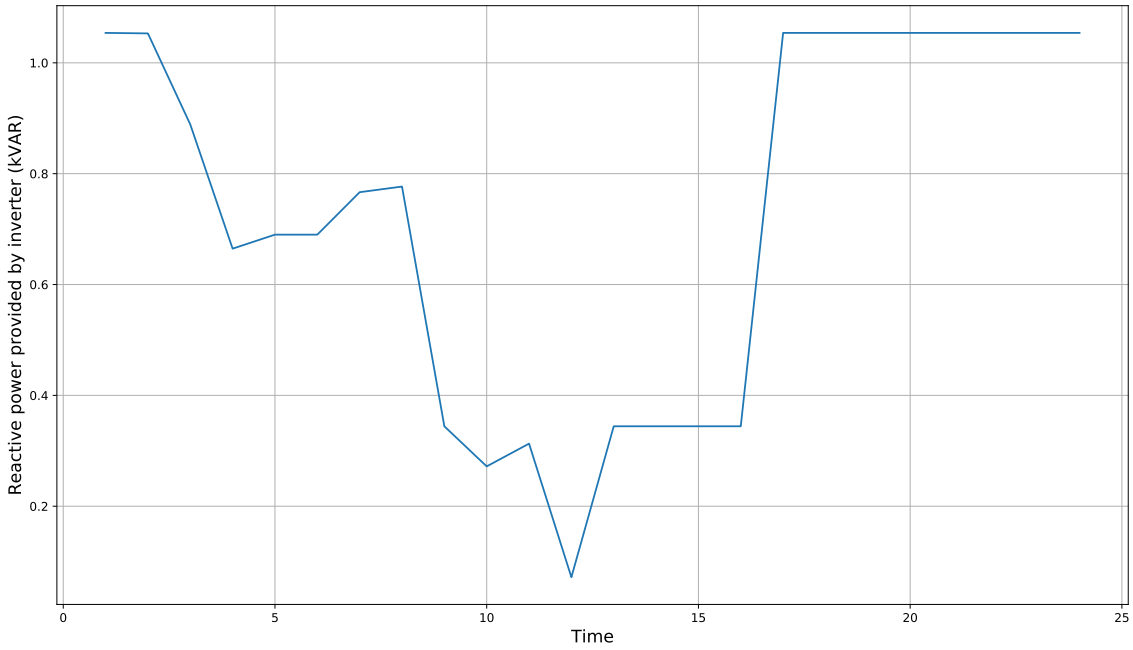

Figure 9: Reactive power provided by the inverter for each hour of the day, base case.

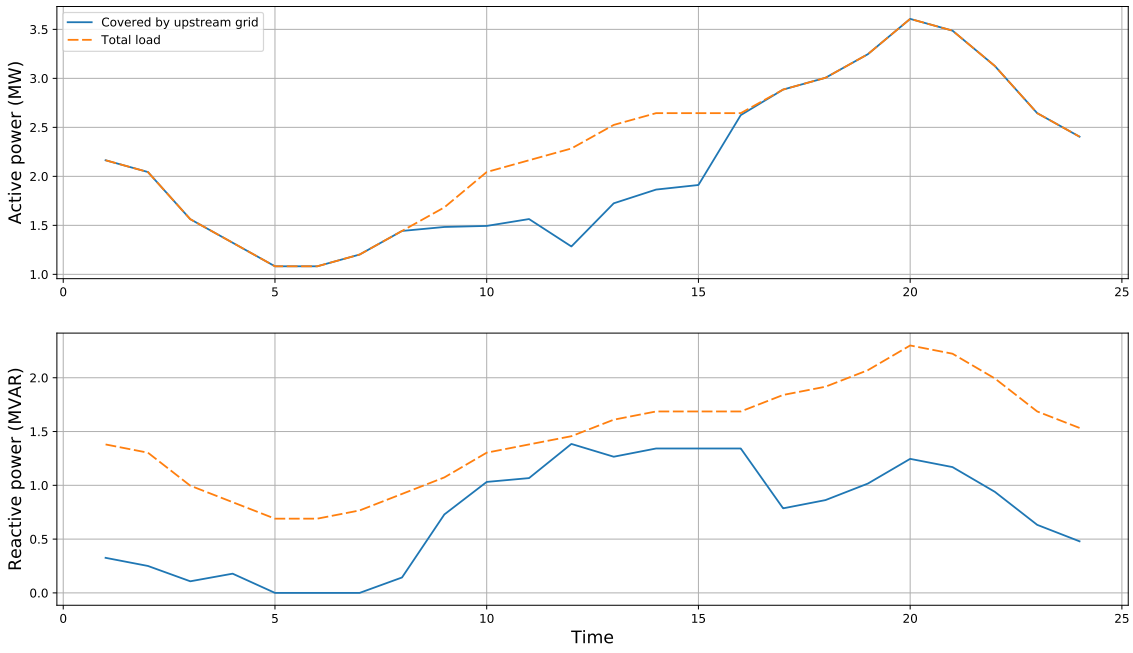

Figure 10: Power covered by upstream grid for each hour of the day, base case.

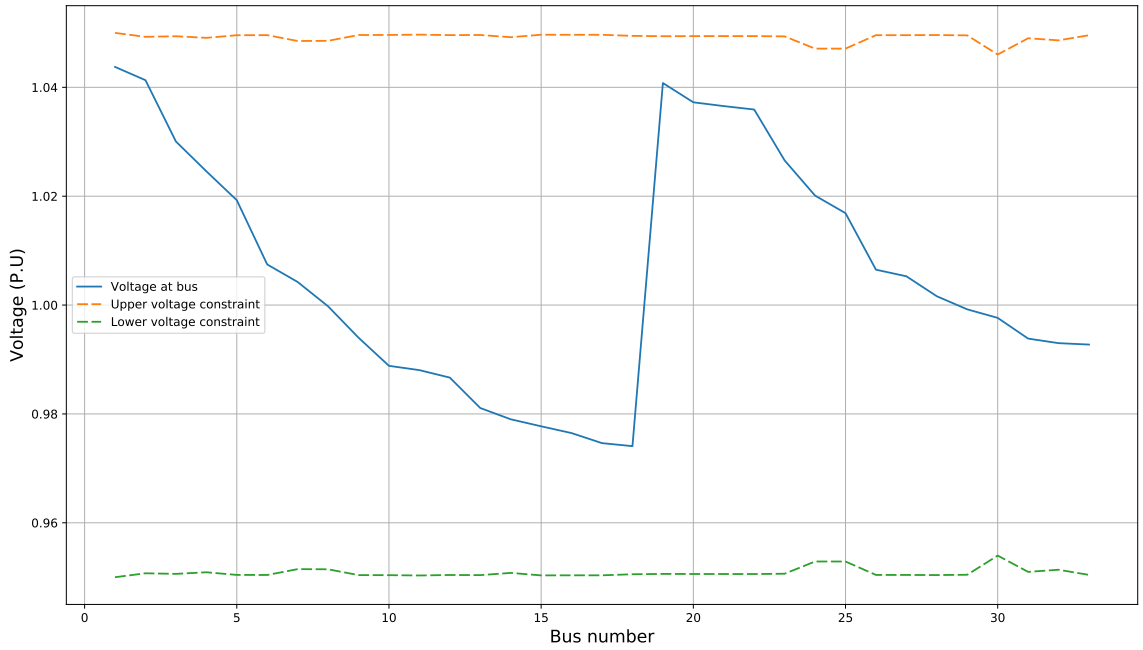

Figure 11: The voltage limits at each bus and actual bus voltage, at peak load, base case.

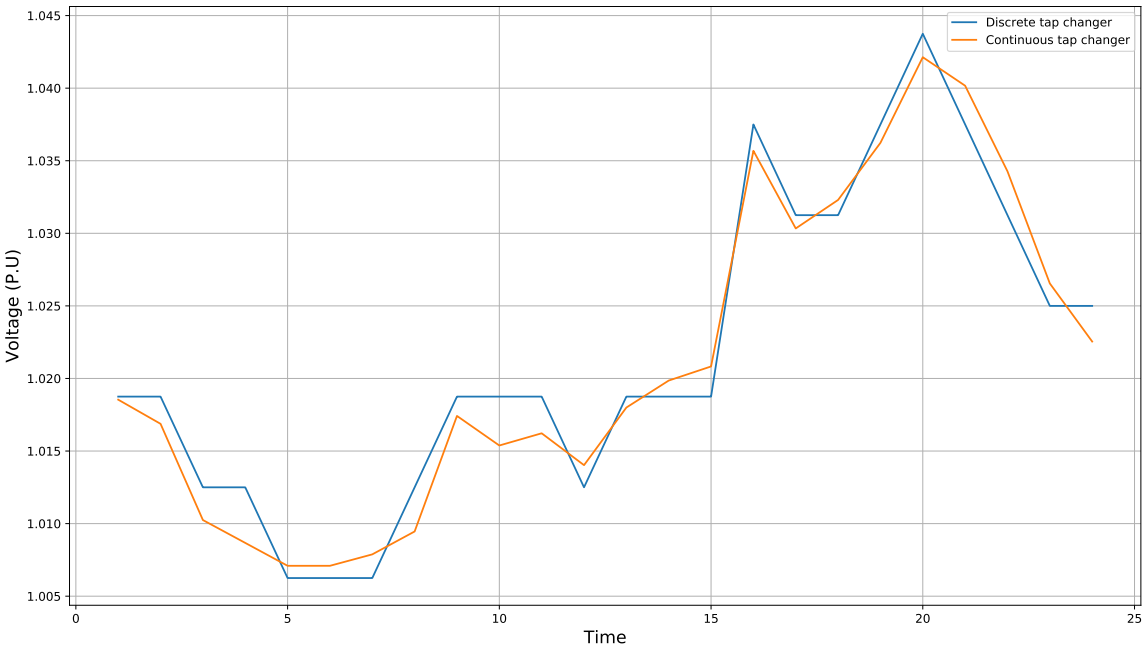

Figure 12: Slack bus voltage at each hour of the day, for discrete and continuous tap changer.

3.1.1 Tap changer modeling

As mentioned in section 2.1.8, the discrete modeling of the tap changer turns the problem into a MILP problem. Table 1 shows a brief summary of some results from the optimization problem using the default discrete option, and using a simplified continuous version. Additionally, figure 12 shows the resulting slack voltage at all time increments using both methods.

It can be observed that the calculation time of the optimization problem decrease with about 25% when moving from the discrete to the continuous model. This is primarily because MILP is somewhat less computationally efficient than regular linear programming. Using a discrete model for the tap changer also yields a somewhat more optimal solution, as can be observed with the value of the objective function. It is, however, important to note that a real tap changer is a discrete system, and thus the discrete modeling will be closer to the realistic "real" values.

Table 1: Comparison between discrete and continuous tap changer modeling.

Method	Calculation time [s]	Objective function [P.U]
Discrete	1.0172	8.2070
Continuous	0.8113	8.0416

3.1.2 Irradiation impact on the inverter capacity curve

As illustrated in figure 4, the chance constrained impact on the inverter is dependant on the active power generated by the PV panels. When there is no generated active power, there is also no uncertainty in the inverter capability. Table 2 shows the different values for $\mathrm{K}(1-\alpha)$ at the hours of PV generation. As expected, the constraints have the highest impact at peak PV hour, and a near negligible impact when generation is low. Intuitively, this means that the total area of the inverter capacity curve is at its lowest value when PV production is at its highest.

Table 2: Time of day impact on inverter capacity curve, $\varepsilon = 0.1$.

Time	9	10	11	12	13	14	15	16
K(1-α)	0.0067	0.0183	0.02	0.0333	0.0266	0.0260	0.0244	0.0007

3.1.3 Forecast error impact on constraints

Adjusting the relative value of the forecast error, ε, is a relatively simple method of observing how the chance constraints are impacted by the quality of the forecast. Figures 13 and 14 show how the acceptable voltage ranges are impacted by changing the value of ε, compared to the base case shown in figure 11 where $\varepsilon = 0.1$.

For the $\varepsilon = 0.01$ case, the chance constraints are almost indistinguishable from a scalar voltage limit. This is to be expected, as a relative forecast value of 0.01 represents a nearly perfect forecast. However, increasing the value of ε from the base case will drastically alter the voltage constraints. At $\varepsilon = 0.252$ the voltage constraints are at the limit of what the base system can handle, meaning that the optimization problem is infeasible for $\varepsilon \geq 0.252$. As an illustration, figure 15 shows the voltage limits for $\varepsilon = 1$

Intuitively the base case that is simulated with a relative forecast error $\varepsilon = 0.1$, and uncertainty tolerance $\alpha = 0.1$ means that all of the constraints will be satisfied with a probability of 90%. If the forecast error increase while the uncertainty tolerance remains the same, then the limits will tighten to ensure that the constraints remain satisfied with the same probability.

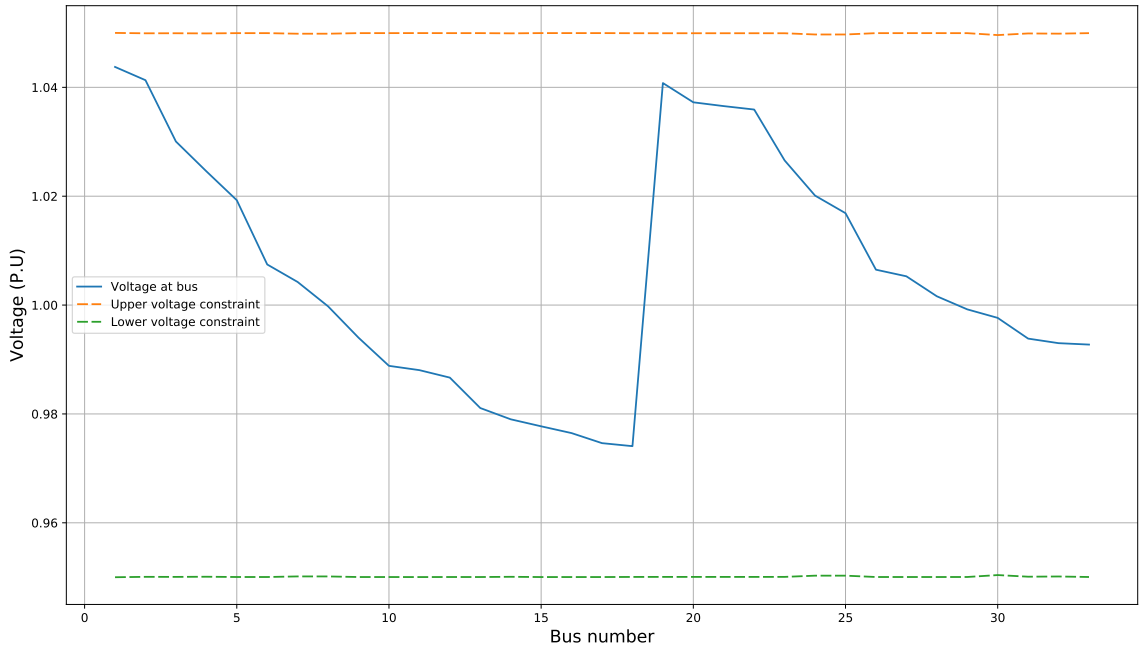

Figure 13: The voltage limits at each bus and actual bus voltage, at peak load, $\varepsilon = 0.01$.

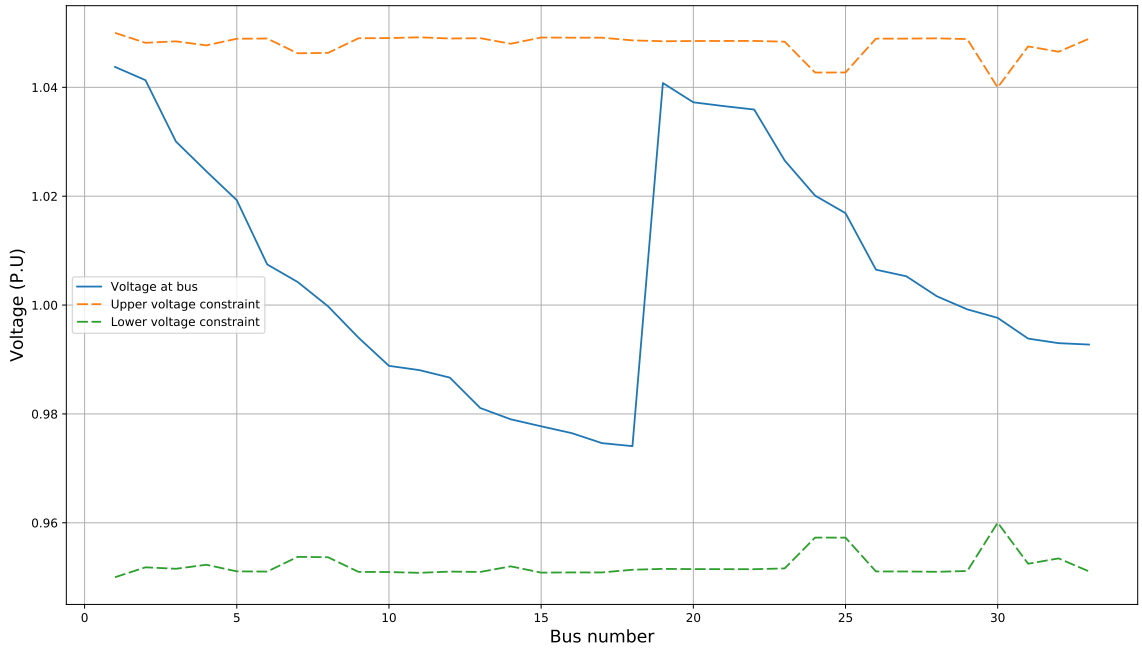

Figure 14: The voltage limits at each bus and actual bus voltage, at peak load, $\varepsilon = 0.252$.

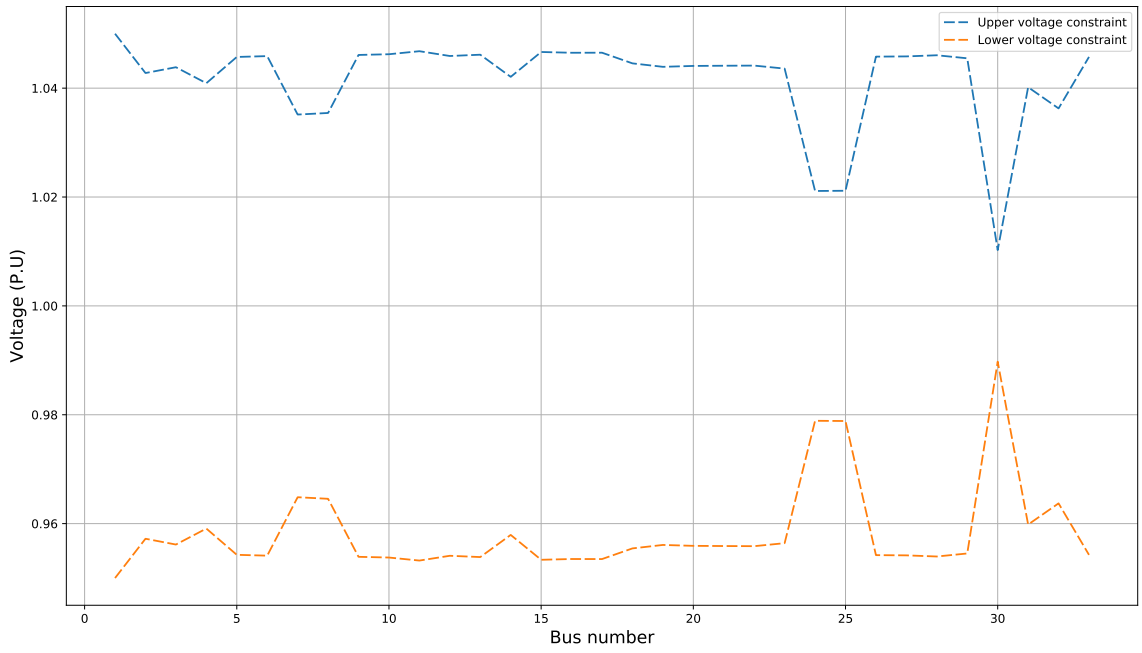

Figure 15: The voltage limits at each bus at peak load, $\varepsilon = 1$.

3.1.4 PV sizing

At the level of installed PV in the base case there is no real concern regarding over-voltage or over-generation from PV, as the total load is still significantly higher than total generation at peak. However, this will change if the amount of installed PV is increased. Increasing the installed PV by more than 2.25 times will violate the system constraints, and studying figure 16 it is easy to understand that this is due to over-generation. As a side note, figure 16 is a good example of the "duck-curve" mentioned in section 1.5.

From figure 17 it can be observed that increasing the installed PV capacity does to some extent improve the overall voltage. This is the same effect as in figure 8, where increased generation at bus 30 means that the slack voltage needs to compensate less for the voltage loss throughout the system. Furthermore, there is a somewhat significant jump in voltage at bus 30 for PV scales larger than 1.5, which can be interpreted as an early symptom of the increased PV leading to over-voltages.

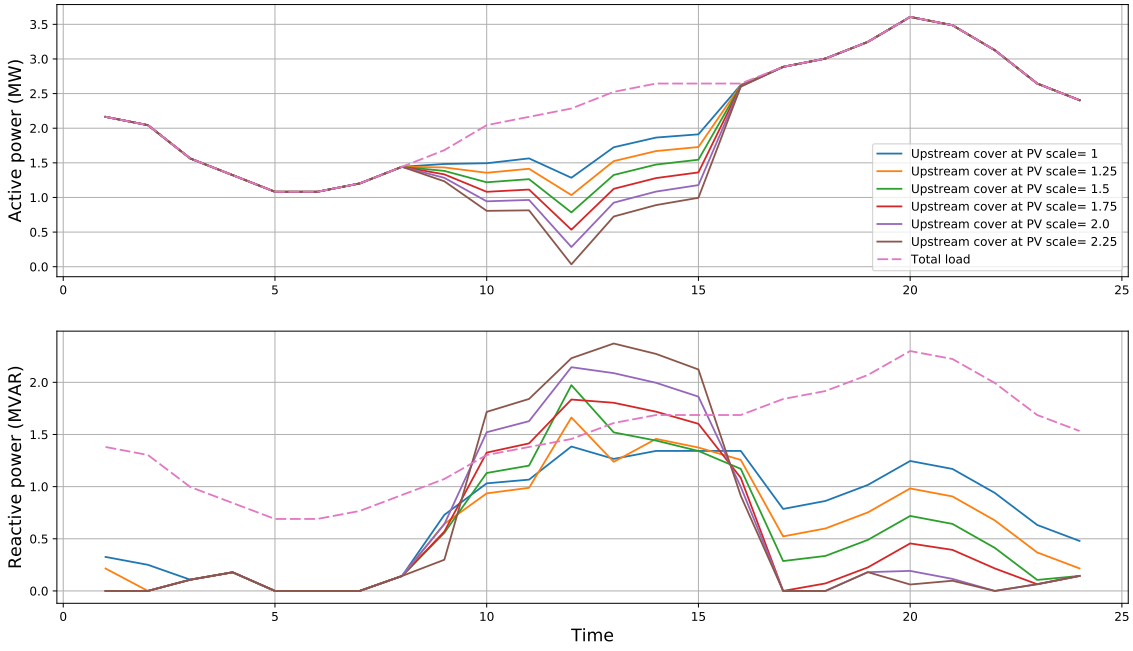

Figure 16: Power covered by upstream grid at each hour of the day, for different amounts of installed PV.

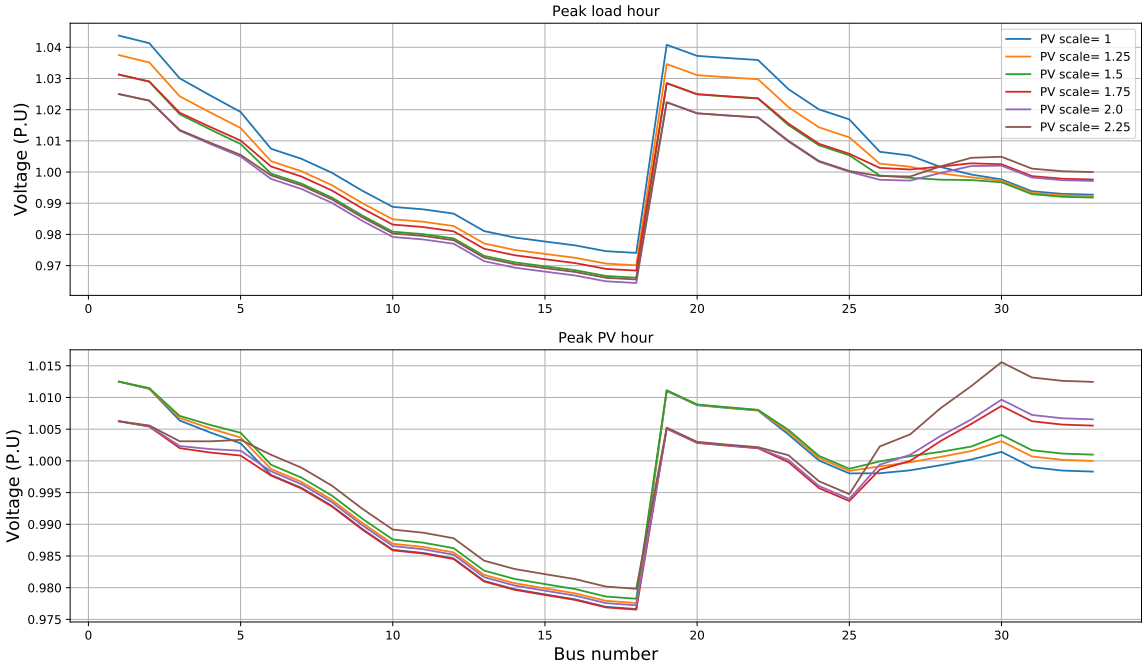

Figure 17: Bus voltage at peak load hour and peak pv-production hour for different amounts of installed PV.

3.1.5 Inverter sizing

It is also possible to imagine increasing the size of the inverter without increasing the amount of installed PV. The inverter should then be able to do reactive power compensation to a greater extent, even when there is maximum PV generation. Figure 18 presents the bus voltage at peak load and production hours for a normal sized inverter, and for a highly scaled up inverter 100 times as large. What can be noted is that while a very oversized inverter does indeed improve the voltage to some extent at peak load hour, there is hardly any difference at peak PV hour.

The objective function of the optimization problem, equations (2.45)-(2.46), is a good indication of how good the total voltage profile is. Looking at figure 19, the change in the objective function for increasing inverter sizes can be observed. The main takeout here is that increased inverter size does decrease the value of the objective function, but only to a certain point. As inverter size reaches 5 times the base case, the objective function stabilize, and further increasing the size of the inverter has no impact on the objective function. Additionally, it can be observed that most of the decrease in objective function happen for the first 2 times of increased inverter capacity.

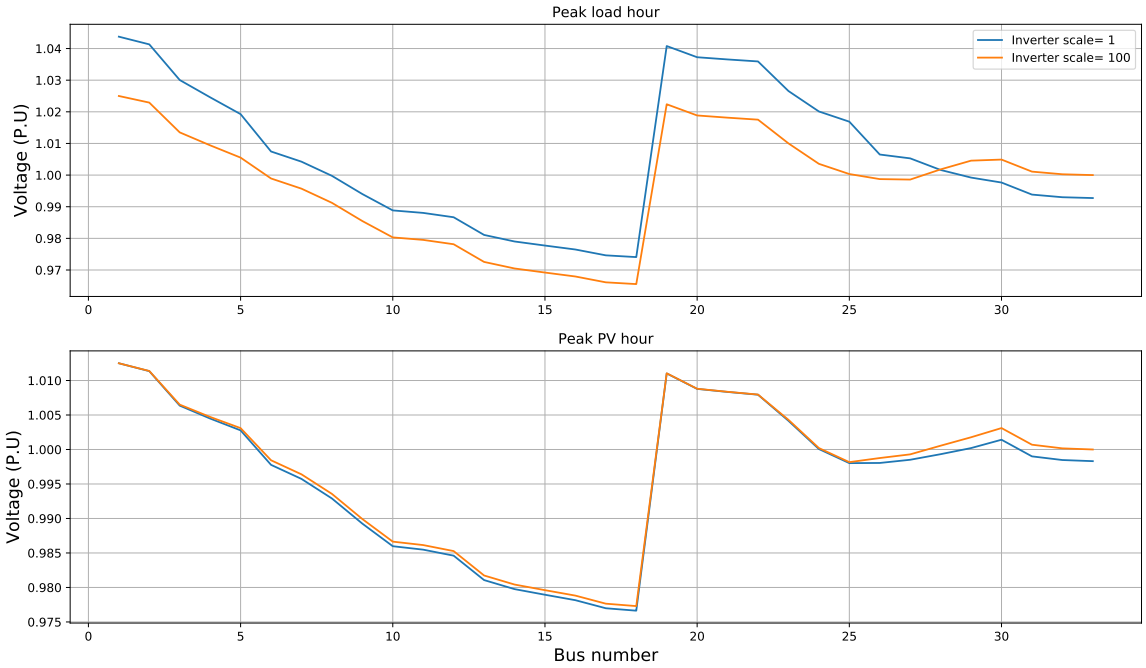

Figure 18: Bus voltage at peak load and PV hours, two different inverter scales.

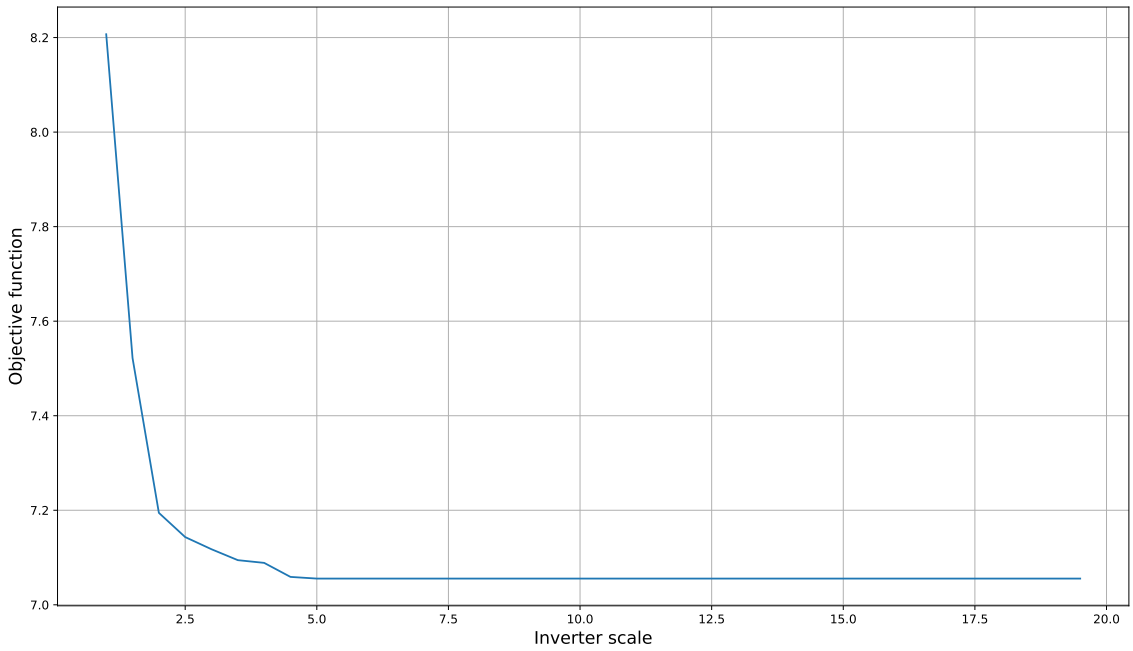

Figure 19: Relation between inverter size and objective function of optimization problem.

3.1.6 Inverter size impact on tolerated forecast error

An additional effect of increasing the inverter size, is the impact it has on the tolerated error in forecasting. As previously mentioned, the base case of the optimization problem is feasible only for forecasting errors of $\varepsilon \leq 0.252$. However, for a 1.5 times increase in inverter size, this boundary is pushed all the way up to $\varepsilon \leq 0.757$. A plot of the voltage limits for this case is presented in figure 20. From this figure it can be observed that the increased tolerance for forecast error can be attributed to smaller peaks in the voltage.

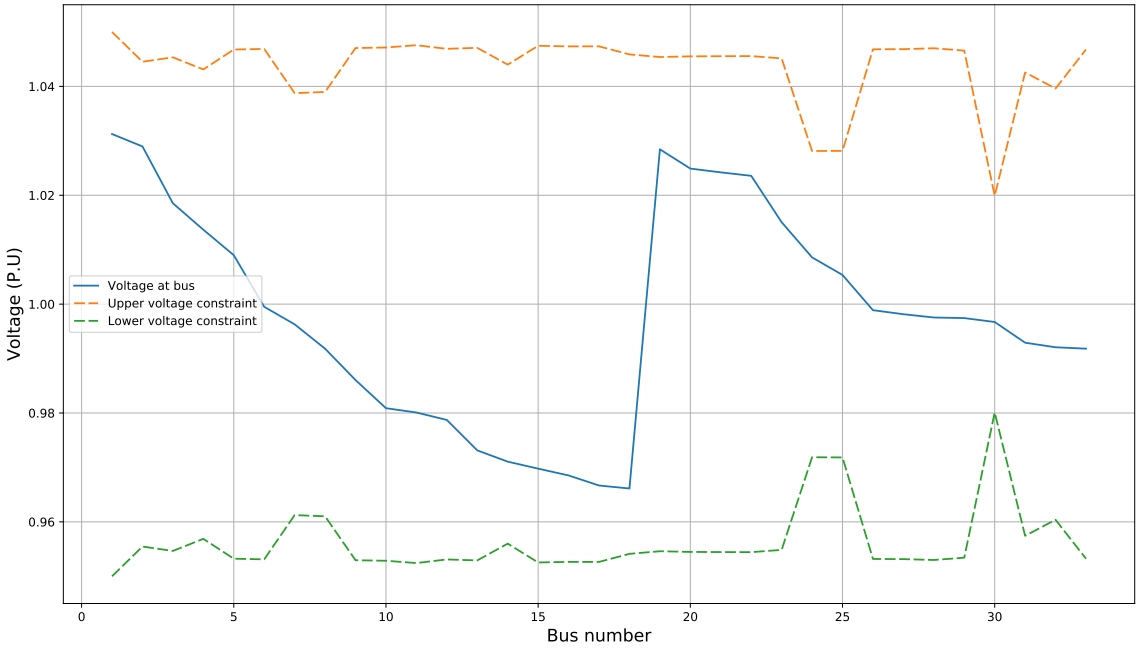

Figure 20: The voltage limits at each bus and actual bus voltage, at peak load, INVscale $= 1.5$, $\varepsilon = 0.757$.

3.2 Adding energy storage

As mentioned in section 3.1, the system without energy storage cannot handle any more PV than an upscale of 2.25 without suffering from over-generation. That is: 2.25 MW installed generation. To cover more of the demand with PV, as well as gaining a benefit of the PV outside of generation hours, a storage system can be implemented. Using the simplified general model described in section 2.1.9 and the data given in 2.2, a generic energy storage system was added to the base case system.

Figure 21 presents the equivalent of figure 8 with storage implemented. It can be observed that even without installing more PV, the voltage profile at peak load hour is slightly better. That is: There is slightly less deviation from 1 P.U. The voltage profile at peak PV-production hour is, however, arguably worse. This slight increase in deviation from 1 P.U can be explained by the fact that the objective function of the optimization problem is defined as the sum of deviation over all hours. Thus the total deviation from 1. P.U is still lower when storage has been included.

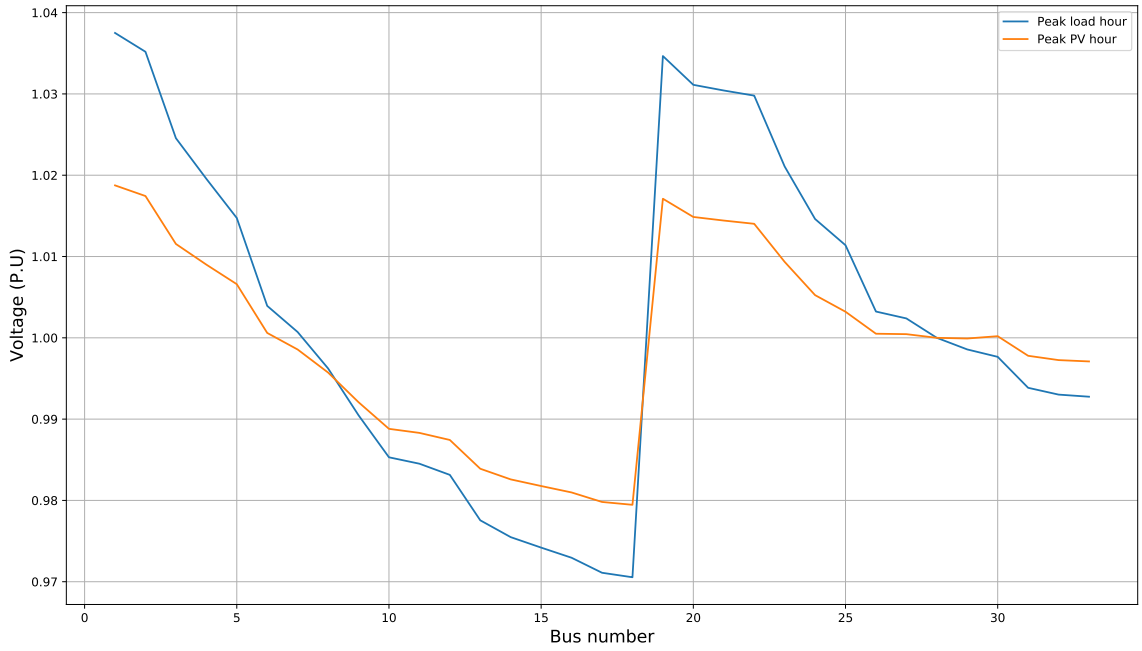

Figure 21: The bus voltage seen at peak load hour and peak PV-production hour, with storage.

Depicted in figure 22 is the active and reactive power covered by the upstream grid, as well as the total demand. Compared to figure 10 from the base case, it can be noted that the upstream grid no longer has to cover all the active power outside of PV-production hours. However, the upstream grid

has to cover a higher amount of the demand at the hours of PV-production. This effect is because the storage system is charging. One additional effect is that there is a slightly less reactive power being covered by the upstream grid at peak PV-production. Again this is due to more power being used to charge the storage system, thus leaving more reactive power capacity available in the inverter.

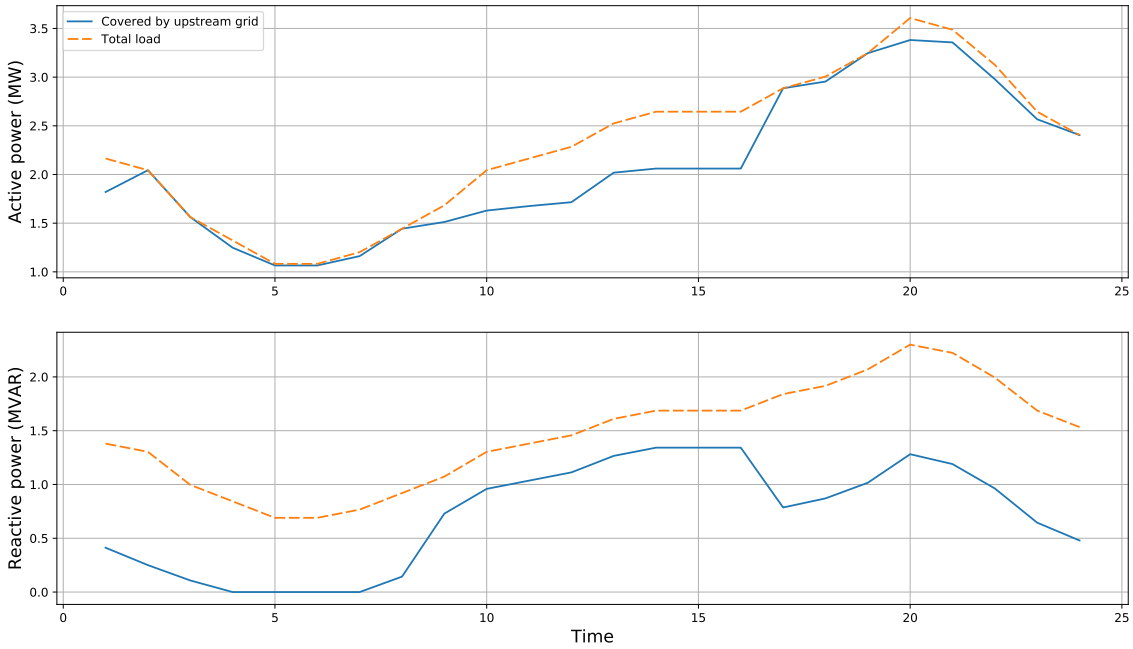

Figure 22: Power covered by upstream grid for each hour of the day, with storage.

Figure 22 can be more easily understood if viewed in combination with figure 23, as this figure presents key data about the storage system. What can be noted is that the storage system discharges slightly during the night, charges during the day, and then discharges back down in the evening. Most of the energy passing in and out of the storage system also does so during the peak PV and load hours. The result is that the peak active power demand is shaved by approximately 0.5 MW. Had this optimization problem been focused on peak shaving rather than voltage regulation, then this effect could possibly have been more extensive.

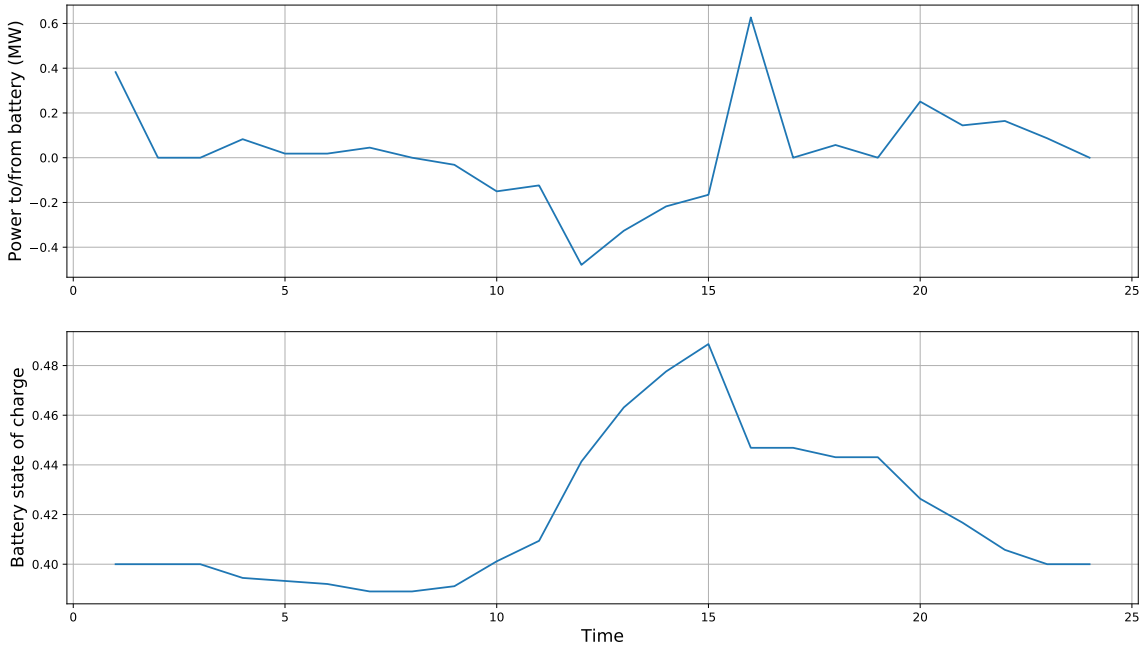

Figure 23: Power to/from storage, and storage SOC for each hour of the day.

3.2.1 Increasing PV capacity

As aforementioned, a major selling point of installing energy storage, is the ability to increase PV-generation. Thus when expanding the system, figures 24 - 27 are the equivalent figures to 21 - 23 where installed PV has been scaled up by 5 times. In addition, $E_{B\,\max}$ has been increased from 15 to 30 MWh to avoid completely filling the storage during the PV-production hours.

Looking at figure 24, it can be observed that the highest voltage peaks have been further decreased, while the lowest voltage value at bus 18 has been somewhat worsened. Additionally it can be observed that the difference between the voltage profiles at peak load and peak PV-production are becoming more similar. Again the total value of the objective function is lower for this case than in the previous case, however, this effect may be hard to discover by looking only at figure 24.

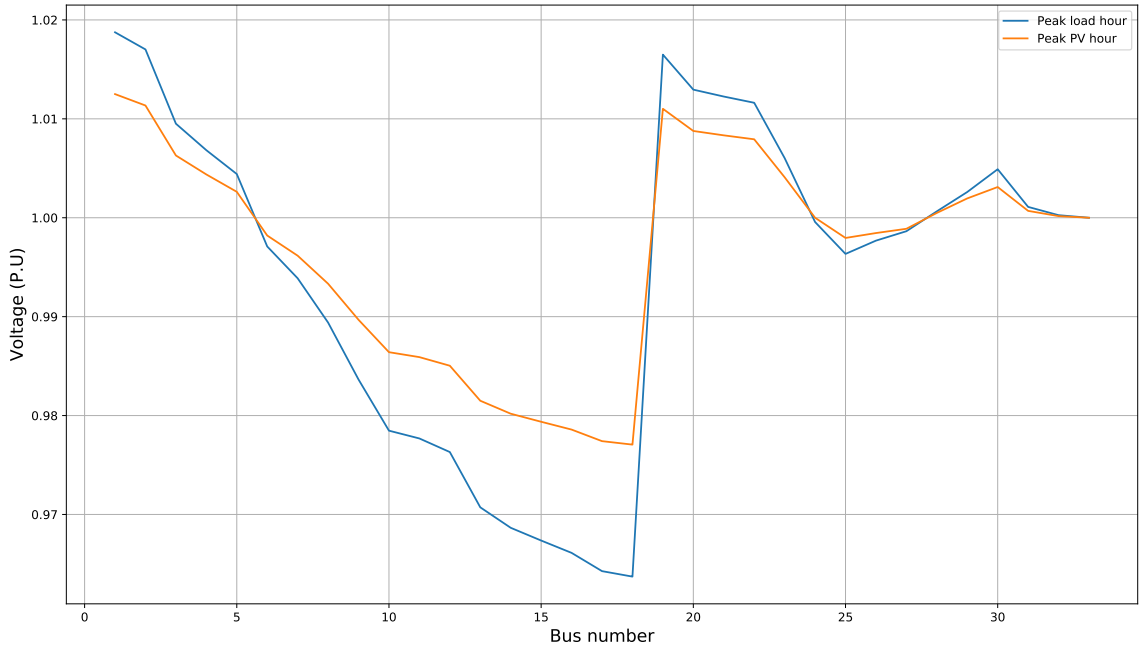

Figure 24: The bus voltage seen at peak load hour and peak PV-production hour, PVscale=5, with storage.

From observing figure 25, it is clear that the demand covered by the upstream grid has changed drastically. There are now large areas of the plot where upstream grid covers very little to zero of the active demand. Additionally, the active power supplied by the upstream grid at peak load hour has been cut by over 1.5 MW.

However, this benefit does come at a cost, which becomes apparent when looking at the reactive power supplied by the upstream grid. The reactive power now varies frequently from very high values, to close to zero values. For time periods with high PV supply to the grid, the reactive power supplied by upstream increase to well over the reactive demand of the other buses. While the storage is charging, however, the upstream demand for reactive power is virtually zero due to the now large scale inverter.

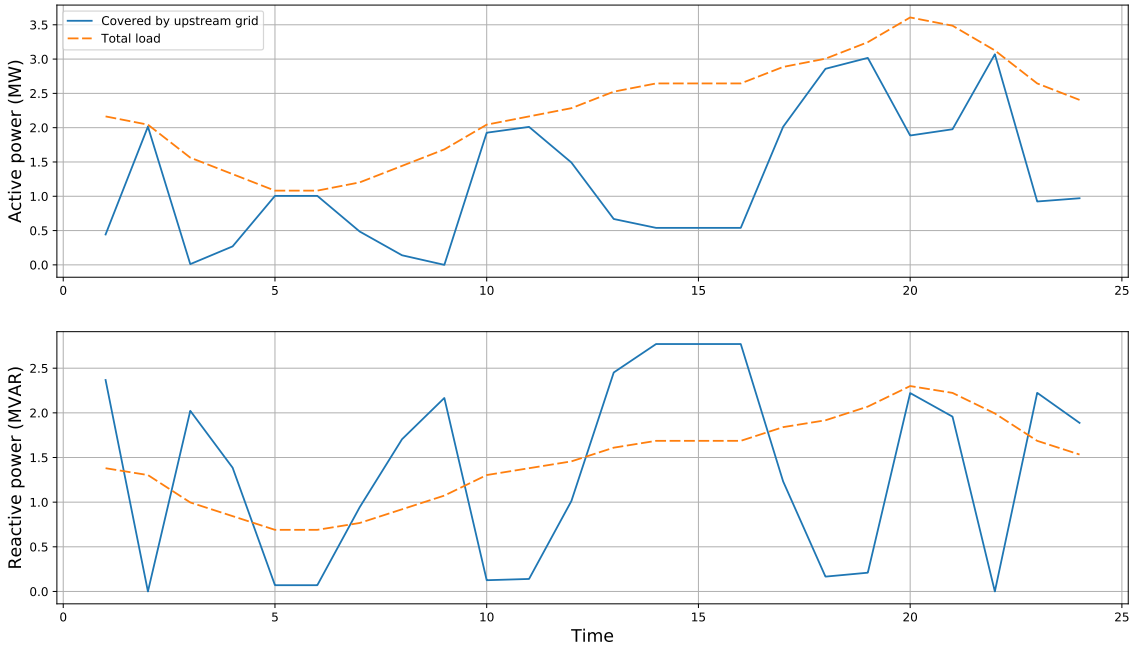

Figure 25: Power covered by upstream grid for each hour of the day, PVscale=5, with storage.

The reason for the large reactive power demand is that the inverter absorbs large amounts of reactive power to counteract the active power injection. The reactive power absorption is so large that the upstream grid has to cover the difference. This turn of events is because the optimization problem objective is to improve voltage profile by all available means. Figure 26 instead show a hypothetical example where the single objective of the problem is rather to minimize reactive power covered by upstream grid.

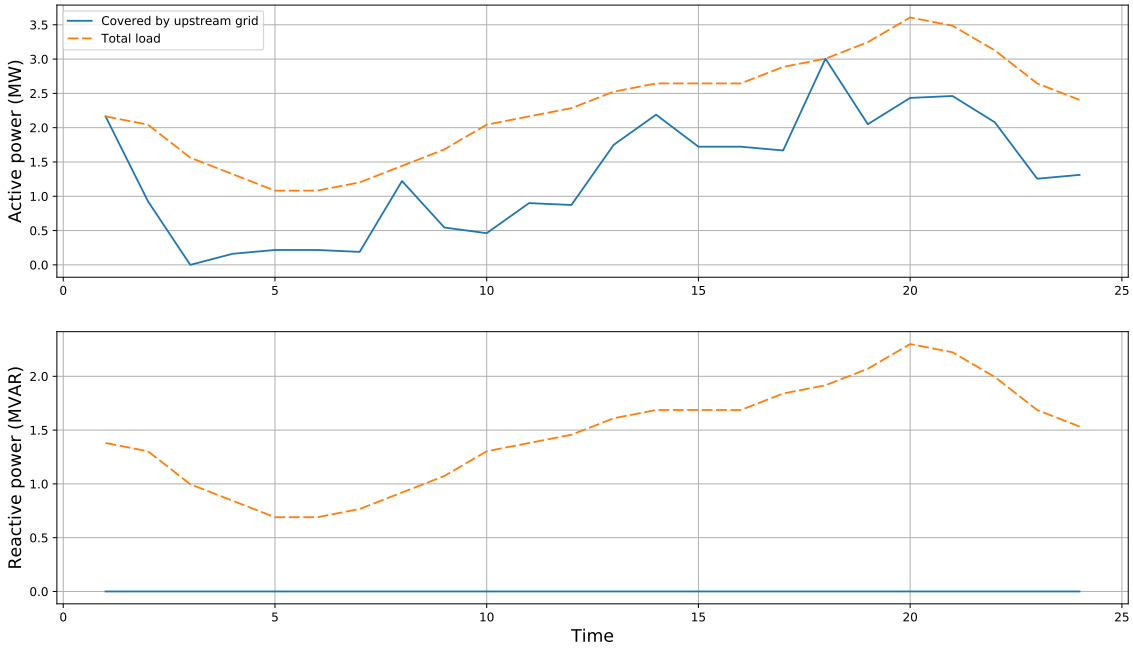

Figure 26: Power covered by upstream grid, PVscale=5, with storage, Q from upstream minimized.

The storage data presented in figure 27 shows that even with the expanded capacity, the storage system can get somewhat close to both full discharge and full charge in a single day. During PV-production hours, the storage system charges from a state of charge of 0.2 to a state of charge of 0.75. For a 30MWh storage system, this is equivalent of charging and subsequently discharging a total of 16.5MWh. With a roundtrip efficiency of $\eta = 0.9$, this means that of the 16.5MWh charged this day, 1.65 MWh will be lost.

In figure 28, the results from figure 11 have been plotted for the expanded PV and storage system. It is quite noticeable that although the voltage constraints are unchanged, the actual voltage at the buses is more comfortably placed within the boundaries in this case. As previously mentioned, the objective function of the optimization problem is a good indication of how overall good the voltage profile is.

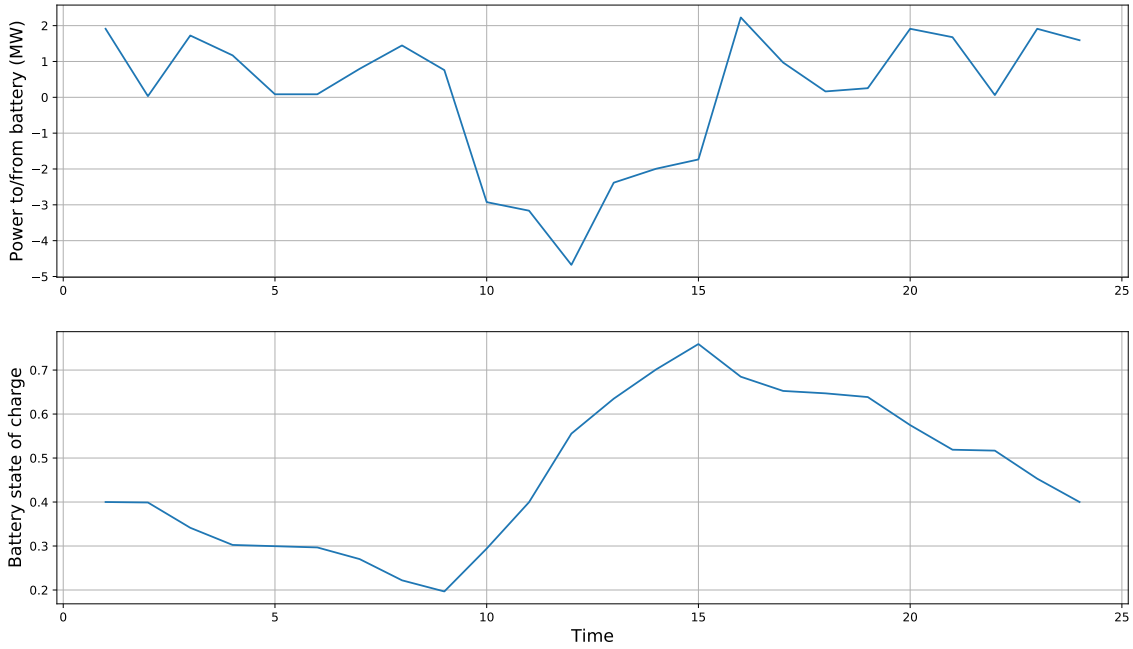

Figure 27: Power to/from storage, and storage SOC for each hour of the day, PVscale=5, $E_{B\,\max} = 30\,\mathrm{MWh}$.

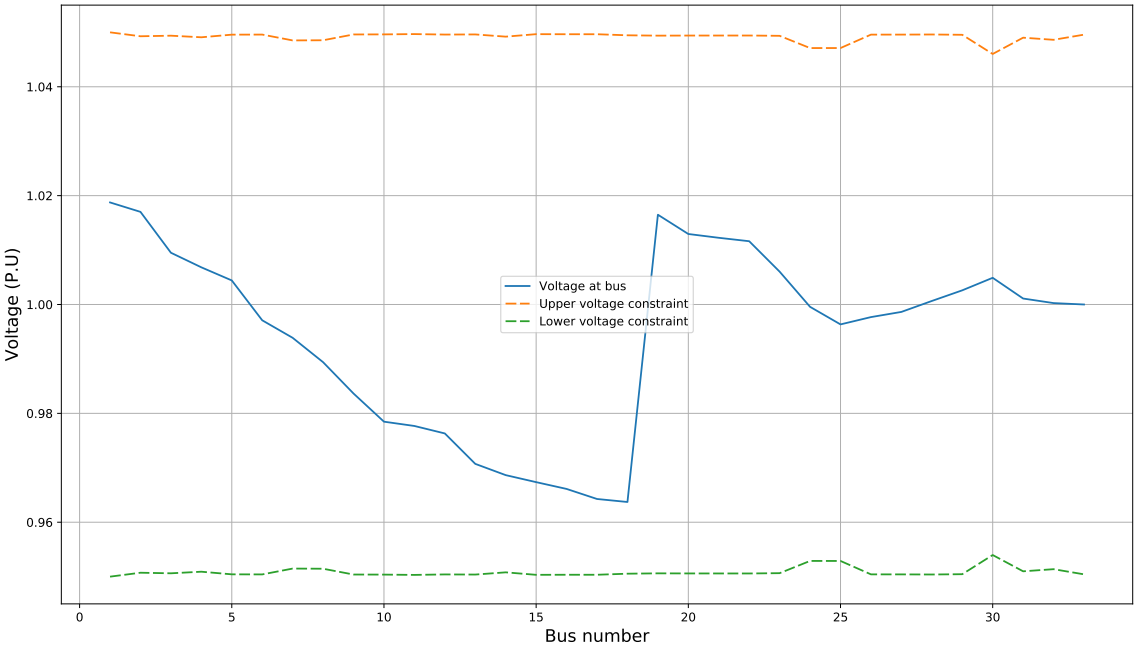

Figure 28: The voltage limits at each bus and actual bus voltage, at peak load, PVscale=5, with storage.

Observing figure 29, it can be noted that the objective does indeed keep declining in value for increasing installed PV. Thus if perfecting voltage profile is the only concern of the operator, then increasing PV-generation and storage is a good basis for doing so. However, there is some indication that the objective value starts to flatten around 8 times increase, and the impact is significantly higher for the first 100% of increased capacity.

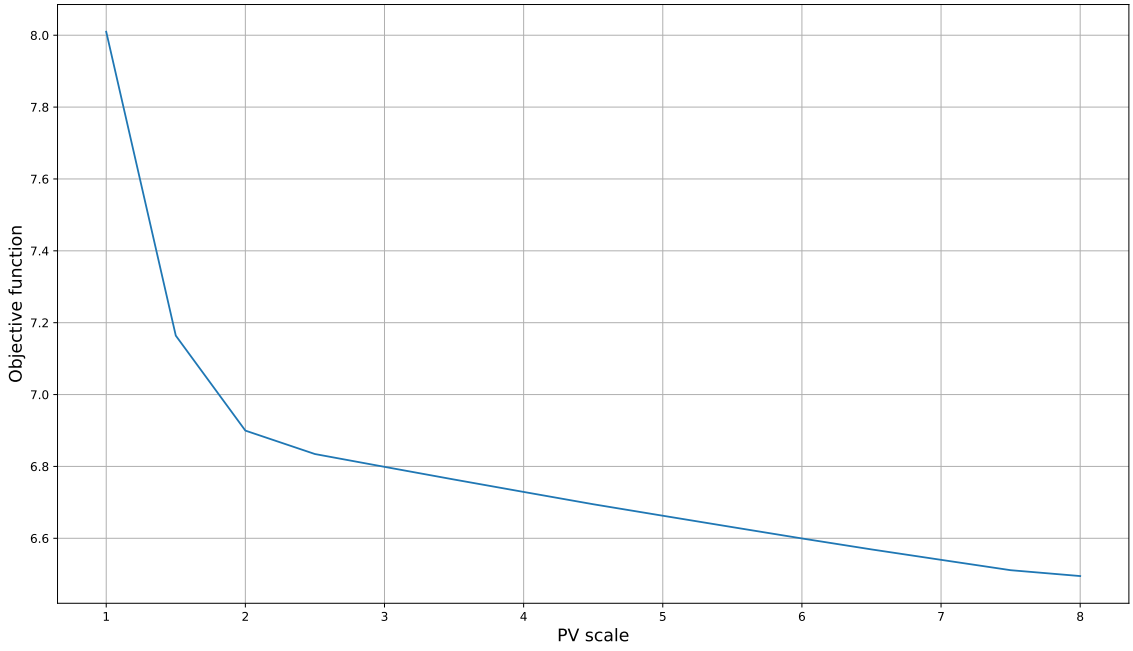

Figure 29: Development of objective function of the optimization problem for installed PV capacity.

3.3 Decentralizing PV generation

Instead of increasing the installed PV at bus 30, it is also possible to expand the system by installing PV and storage at multiple different buses. Thus instead of scaling up the capacity at bus 30 beyond the base case, the optimization problem was rerun with buses 14, 21, 24 and 30 as PV-buses. Each PV-bus had a 1 MW PV unit and a 1.054 MVA inverter. Furthermore, each bus had maximum storage power $P_{B\,\max} = 3$ MW and maximum capacity $E_{B\,\max} = 9$ MWh. The resulting voltage profile and storage behavior can be seen in figures 30 and 31 respectively.

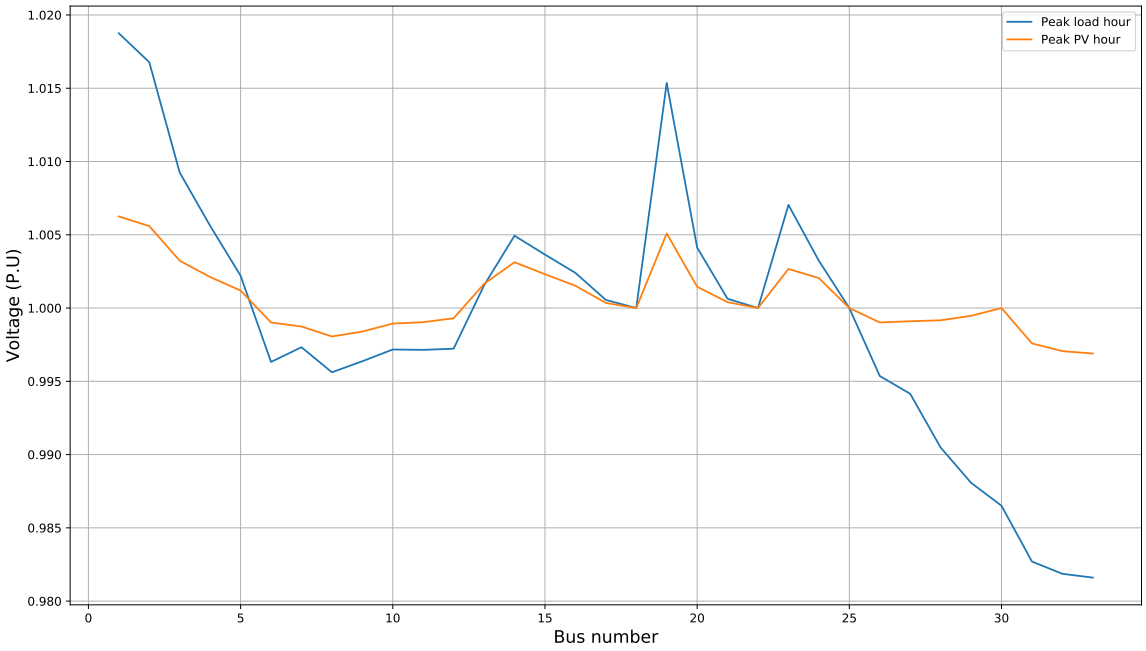

Figure 30: The bus voltage seen at peak load hour and peak PV-production hour, decentralized PV + storage.

Inspecting figure 30, it becomes immediately clear that the overall voltage deviation of the system is significantly reduced. Furthermore, both peaks and lows are closer to 1 P.U. The previously most challenging bus, 18, now has a voltage of almost exactly 1 P.U, while voltage at slack bus is kept below 1.02 P.U. Looking at figure 31, it can be observed that the storage at bus 30 now does no work outside of generation hours, while all the other storage systems do significantly more. The impact decentralization has on the power supply from upstream grid can be seen in appendix C.

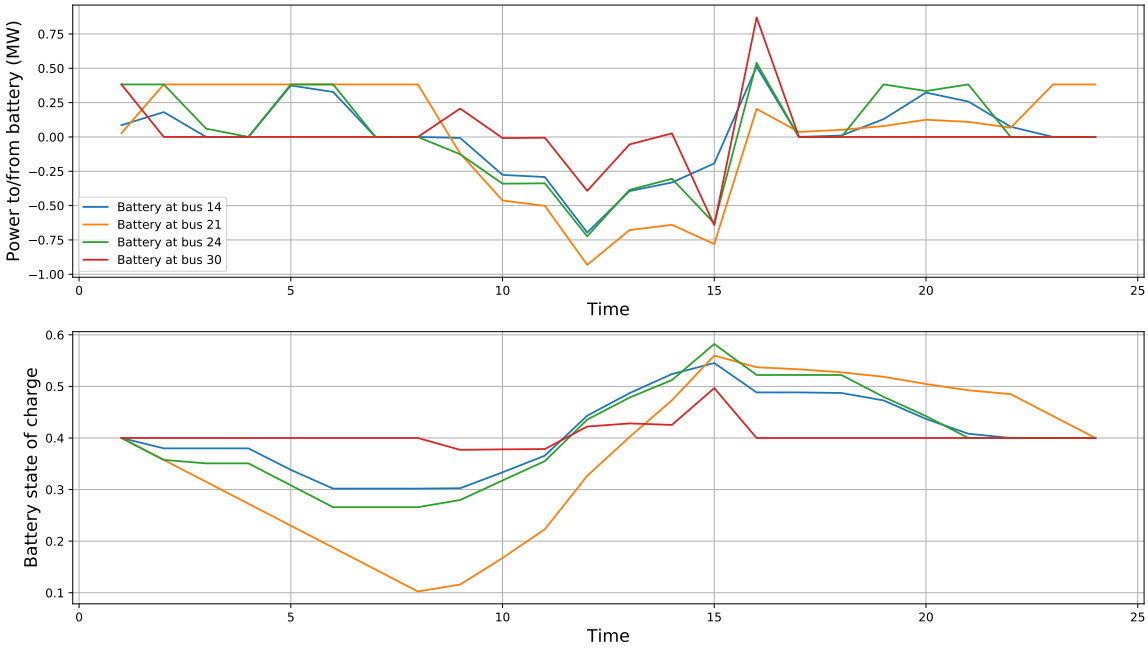

Figure 31: Power to/from storage, and storage SOC for each hour of the day, decentralized PV + storage.

3.4 Distribution grid without PV

To get a better understanding of how the distributed PV system impacted the distribution grid, optimization was also run on the grid without any PV. In other words bus 30 was treated as any other bus, and all demand was covered by the upstream grid. The resulting voltage profile at maximum and minimum load hours can be seen in figure 32. It can be easily observed that the voltage profile at peak load is worse than the case with PV, and significantly so compared to the case with expanded PV and storage.

Table 3 shows the value of the objective function for the different optimization problems run, and further shows the significant positive effect of the distributed PV and inverter on the voltage profile. The small difference in objective function between the base case and the base case with storage, further proves that there is little benefit in installing energy storage if the PV system is too small to contribute to over-voltages. Meanwhile, it is important to note that this model only consider voltage over 1 hour time steps, and not rapid generation fluctuations from e.g passing clouds. The table also shows the huge improvement that comes from decentralizing the installed PV.

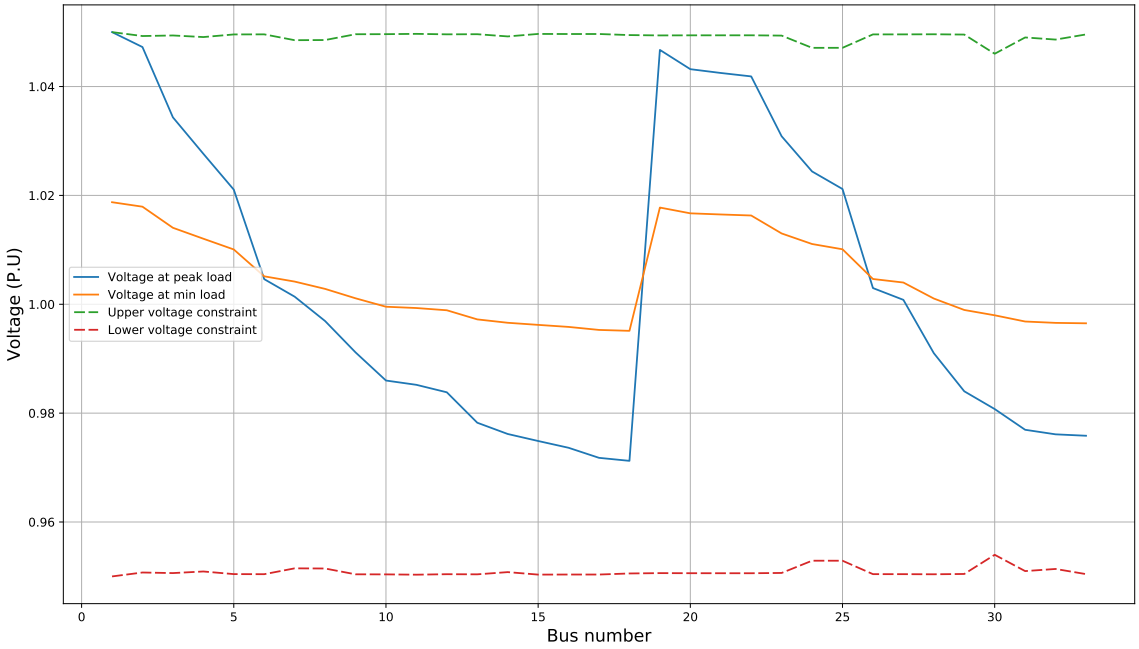

Figure 32: Bus voltage limits at max load, and actual bus voltage at max and min load, no PV.

Table 3: Value of the objective function for the different optimization problems.

System	Normal grid	Base case PV	PV + storage	5·PV + storage	Decentralized PV+storage
Value of objective function [p.u]	11.687	8.207	8.010	6.663	2.217
Improvement from normal /bus/time [p.u]	n/a	0.0044	0.0046	0.0063	0.012
Computation time [s]	0.75	1.02	2.90	1.21	10.04

4 Discussion

This chapter will discuss the implications of the result obtained in the last chapter, and validate the results. Section 4.1 will discuss the information gained from the optimization scenarios, looking first into the overall results, and then into the impact of the different changes to the system in sections 4.1.1 - 4.1.5. Section 4.2 look at the viability of the model, what simplifications have been made and how do they impact the model. Subsequently, sections 4.2.1 - 4.2.7 will handle separate aspects of the model, and discuss shortcomings and potential improvements.

4.1 Information gained from the optimization

The value of the objective function is calculated from equations (2.45)-(2.46), and represents the sum of the deviation from 1 p.u for all buses over all time increments. Thus, this value is an indication of the total system performance. Inspecting the value of the objective function for each of the main scenarios that were optimized, which is presented in table 3, two main observations can be made: The system performance improves for each upgrade of the system, and the different system upgrades have vastly different impact on that change.

The by far biggest impact on the system is the change from centralized to decentralized PV, while the introduction of storage to the non-decentralized case has an almost negligible impact on the voltage profile (an average of 0.00025 P.U improvement per bus per time).

Looking at the results as a whole, there is no doubt that the distributed PV system improves the voltage profile of the distribution system. This is both a result of the active power injection at bus 30 when there is PV-production, but also the inverter connected to the PV doing reactive power control during and outside of production hours as seen in figure 9.

The well known problem with over-voltage at PV buses is not present for the base case. This can be primarily attributed to the amount of installed PV capacity in the base case. At peak production for the base case, the production is still only 1 MW, which even in the middle of the day is less than half of the demand. Thus it is easy to conclude that over-voltage will not be a real problem for this system until a higher PV capacity is installed.

4.1.1 Impact of installing storage in the base case

Since the base case system is at no time covered entirely by PV, there is also no need to curtail over-generation in the base case. Thus, purely based on getting everything out of the installed PV, it is superfluous to install storage. That conclusion does, however, not account for any grid benefits of saving the power for later. Considering that most energy systems will see an increase in energy cost for increasing demands, it is quite possible that it can be economically profitable to rather use power from the upstream grid during mid-day. Thus, the PV generation can be stored and used to shave demand peaks during the evening.

Some peak shaving can be seen in figure 22, where storage has been implemented into the base case. However, it is important to note that this problem has been optimized purely based on improving the voltages. The system still sees it as beneficial to shave the peaks, however, this decision is based on reducing the transmission losses that affect the voltage. The peak shaving would have been much more visible if there had been added a cost of upstream generation to the model, and if the objective was to minimize cost.

As mentioned in section 1.5, PV generation has a marginal cost of practically zero. Thus it can be very favorable to use stored PV for peak shaving. Economically, this is especially true in systems with a high dependency on non-renewable dispatchable generation like coal or gas.

Whether it is economically viable to install and use PV+storage in a given distribution system is, ultimately, a decision that has to be made considering many factors: The levelized cost of electricity for a new PV system, the cost of the upstream dispatchable generation, how much there is to gain on reducing line losses (is the system strained or not). However, this will not be discussed here at length, as voltage regulation is the primary concern of this thesis.

4.1.2 Impact of PV sizing

With any renewable energy source, it is desirable that as much of the total energy consumption as possible is covered by it. As mentioned in the results, installing storage gives an opportunity to increase the installed PV as well. Increasing the installed PV to five times that of the base case has some significant effects on the system: The deviation in voltage from 1 P.U is further decreased, and the difference between voltage at peak load and peak production is also decreased. This decrease in difference between peak hours can be mainly attributed to the stored PV shaving the peaks.

As improving overall voltage profile goes, the increase in installed PV is purely beneficial. The only significant disadvantage is that the voltage at bus 18 is lower for this scenario. As bus 30 contributes more to the voltage of the other buses, the maximum voltage at the tap changer can be lower while

still keeping the rest of the bus voltages close to 1 P.U. As a consequence, the voltage at bus 18 deviates slightly more from 1 P.U. while the value of the objective function still decrease. It is worth noting, however, that voltage at bus 18 is still within the constraints.

When it comes to the flow of power in the system, the increase in installed PV results in some disruptive changes: The upstream grid now has to cover significantly less of the total demand for active power, in fact during hours 3 & 9 it supplies no active power at all. Additionally, the highest amount of active power covered by the upstream grid is now at hours 19 & 22, since required power at hour 20 has been decreased by over 1.5 MW.

Meanwhile, the large leaps in active power delivered from the PV and storage system has a large impact on the demand for reactive power. Comparing figures 25 and 26, there is good reason to evaluate how realistic the model is when only focusing on voltage regulation. This does not mean that minimizing reactive power delivered from the upstream grid is a better objective, but delivering reactive power does not necessarily come without a cost. Especially considering the on/off behavior of the reactive power shown in figure 25.

4.1.3 Impact of decentralizing PV

Decentralizing the PV from one bus to four different buses was shown to be the single most effective change to the system in terms of minimizing the objective. This is an interesting result, as the total PV and inverter capacity actually decrease somewhat from the PVscale=5 scenario (5 MW to 4 MW). The primary reason why it is so effective is that the PV-buses have been strategically placed so that every radial has a voltage regulator. In addition, no bus is more than 6 buses from its closest voltage regulator. Thus the overall voltage loss due to line impedance is decreased.

When the regulators are placed closer to the place of demand, it is less necessary to compensate for voltage loss in the lines. Thus the voltage can be closer to 1 P.U, while at the same time decreasing total power loss. As there is no real limit to how far this can be scaled, the voltage could potentially be almost perfect if every bus was equipped with a PV and storage system. At least as long as there is sufficient capacity to power the grid, and sufficient storage to avoid over-voltages.

The obvious downside to such an expansion is the cost of investing in distributed PV at such a scale. Certain components like the inverter will be cheaper as one large unit, rather than several smaller units with the same cumulative capacity. The same can be said about installing and maintaining PV-panels and battery banks at several different locations. Ultimately a decision made about a real system will have to weigh the cost of such an investment versus the benefit of an improved voltage profile.

An additional factor to be considered, is that control over the regulators is still centralized. Centralizing control is by far the easiest way to maintain control over the voltage, but it does require some form of communications infrastructure. That infrastructure could be the internet, although connecting critical infrastructure to the internet is associated with security risks on its own. The alternative is that each regulator is autonomous, which can lead to different regulators working against each other.

Lastly it is worth mentioning that the computation time increase drastically for the decentralized case. A simple explanation is that a normal bus has two equations describing active and reactive generation at the bus, while a PV-bus is constrained by 15 different equations describing the active generation, the inverter and the battery. This is unchanged if the single installed system is simply scaled up, but adding 3 new PV-buses equals to $15 \left[\frac{\text{equations}}{\text{h}}\right] \cdot 3 \cdot 24 \, [\text{h}] = 1080 \, [\text{equations}]$ that are added to the optimization problem. The amount of equations will thus increase linearly with the amount of PV-buses.

4.1.4 Impact of inverter sizing

Increasing only the inverter in the base case was shown to have an impact on the value of the objective function. However, the system does, as shown, reach a point around 5 times increase where just adding more capacity to the inverter has no further impact on the objective. Increasing the capacity of the inverter will expand the capacity to perform reactive power control, and as such it is a good way to illustrate the impact that pure reactive power control has on the system voltage. However, it is worth noting that installation of vastly oversized inverters is not something that is actually done in any real system.

In a real system, large scale reactive power control would be done by dedicated components such as switched capacitors or a static synchronous compensator (STATCOM). While switched capacitors are more simple, a STATCOM is based on a power electronics interface. Thus it can function much like an oversized PV inverter, although more specialized for this purpose. However, as mentioned in section 1.5, reactive power control is usually not applied in distribution systems at all. The primary reason rective power control is considered as an option for systems like this one, is that the inverter is already required to install the PV, and thus might as well be utilized fully.

Another important aspect of inverter sizing is the initial assumption of an oversized inverter. The inverter is by far the most expensive single component of a PV system. Even on a sunny day, the PV panels will not produce at potential maximum power for most of the day. Thus having an inverter that is capable of handling more power than the system will ever produce, is not profitable in it self. The benefit gained from an oversized inverter is primarily attributed to the system operator, and there would have to be some kind of other incentive if a private consumer were to install an

oversized inverter with their PV system.

4.1.5 Impact of chance constraints

It is important to realize that there is nothing inherently random about chance constrained optimization. Rather, CCO is an optimization tool that makes it possible to model an uncertainty in the parameters used. For a system like this one, this means that although load and solar irradiance for the next day is uncertain, it can still be optimized within a quantifiable probability. The important limitation for that probability is that a forecast is available, and it has been decided by how much the forecast can be wrong.

As previously shown, an increase in the forecast error results in more narrow voltage constraints. Continued increase in the forecast error will result in the system no longer staying within boundaries, and for the base case system this happened at $\varepsilon = 0.252$. Intuitively that means that at any point of the simulation, the load or the solar irradiation may be 25.2% higher or lower than the expected value. The fact that the system cannot keep within boundaries does, however, not mean that such a system would never work under those conditions. What it does mean, is that we cannot with α certainty say that it does.

A major advantage of using CCO for this optimization problem, is that we can easily decide what margins we want to run the system with. Thus it is easy to see how the system is impacted by less certain forecasts (ε), or higher demanded certainty(α). Since the chance constraints are connected to the voltage at each bus, it is also easy to see which buses are the most vulnerable to forecast error. Thus the potential error is not dealt with, but rather the risk is quantified.

In the expanded system cases, the voltages are mostly further within the constraints. A good example of this can be seen for the case in figure 20, where a 50% increase in inverter capacity means that the system is feasible up to a forecast error of $\varepsilon = 0.757$. Thus an investment in increased capacity is not only a matter of better overall voltage profile, but in fact an investment that can be made to decrease the impact of uncertainty. In short: Investing in increased capacity can be considered as the cost of certainty.

4.2 Viability of model

4.2.1 The size of the time increments

As aforementioned, the optimization in this thesis was done with relatively large 1 hour time increments, which entails some distinct advantages and disadvantages.

Most importantly there are no transients in the model at all, and as such this is a purely stationary set of optimization problems. One major issue with a purely stationary solution, is that it fails to model the often fast intermittency of PV generation. If a patch of clouds were to drift over a PV installation, then that could more than halve the generation for just a couple of seconds. After the clouds disappear the generation would suddenly spike again, which could lead to short time overvoltages. This behavior is impossible to model when the irradiation is treated as constant for one hour at a time.

The intermittent behavior of PV is often a major reason to install energy storage, which is not something that can be interpreted from the results presented here. In fact tap changers may have a response time of multiple seconds, which may lead to severe voltage irregularities when a large amount of PV suddenly stops generating. In such as situation, the voltage can be held stable by a storage system until the PV stabilize, or the tap changer adjusts. These are operations that don't impact the SOC of large storage systems to a large degree, but can be vital for the voltage stability. In this model, however, energy storage is purely used to save energy for later use.

Since the model is stationary for each time increment, there is no modeling of the transient response of different components. In fact, there is no specific mention of specific components at all. Every component used is presented as a generic component with generic values. The inverter is just defined by its maximum rating, PV panels are defined by their peak power output, and storage is given as a generic storage technology. This is done because the purpose of the thesis is to look at a large scale system, and not the performance of individual components. When everything is stationary, the time dependant performance of individual components is also somewhat less relevant.

Optimization of a stationary system is not inherently worse than a transient one, but it is important to recognize what the model can tell you and what it cannot. In short the impact of the time increments are that:

- The model **does** give realistic values for a stationary distribution system with distributed PV.
- The model **does** give insight into the impact of chance constraints, and how the forecast error impacts the uncertainty.
- The model **does** show the benefits of installing energy storage and storing energy for later

use.
- The model **does not** show the viability of the system for short time intervals
- The model **does not** show anything about how individual components respond to transient behavior

The way the model is formulated it is still possible to run the optimization with smaller time increments, as long as the increments are large enough to avoid transient behavior. However, transient component behavior is not modeled anyway. Thus, there is no indication from these results that any new information would come from decreasing the time increments. Since the amount of variables and equations increase linearly with increased time iterations, simulating the system with one minute increments could easily take 60 times longer. The impact of decreasing time increments is, however, an aspect that should be researched more thoroughly.

4.2.2 Tap changer modeling

In the results, a different simulation using a continuous tap changer for the base case system was shown. While the discrete version better models the behavior of a real tap changer, there is good reason to argue that the discrete modeling is unnecessary. Mostly it can be argued that the extra computation time is not worth it when the difference between the models is so small.

The 25% increase in computation time is completely insignificant when the total computation time is 1 second. However, if the optimization problem was run on a significantly larger system, or iterated over multiple solutions, then approximating the tap changer could potentially be a good choice to decrease computation times. Furthermore, if this optimization was done using nonlinear programming, then doing a continuous approximation of the tap changer could be easily defended, as computation times would increase drastically.

4.2.3 Energy storage modeling

During the modeling of the energy storage, no specific technology has been selected. Instead a generic storage technology with a 90% round trip efficiency was used, which is roughly an average of the relevant battery technologies available for grid storage. Which technology used is not entirely irrelevant, as there are some key differences between them. For instance, there is a big difference between the charge/discharge capacity per battery size for different battery technologies. Lithium-ion batteries can charge much faster than lead-acid batteries, and you would thus need significantly less total storage capacity to cover the same short time power output/input. Again, this aspect would be more important if the time increments were smaller.

The mathematical formulation of the storage was made very simple, so that it could be easily implemented in the existing optimization problem. As a whole the storage is treated as a "black-box", where the model only keeps track on total capacity, power in/out and efficiency. Thus there is some loss of realism, but the model is easy to implement, easy to scale, while still keeping track of losses. As storage modeling or optimization is not the primary objective of this thesis, this can be considered an acceptable compromise.

4.2.4 Line constraints and PV localization

This model does not consider thermal line constraints. As a consequence there is nothing that keeps the line flow from reaching very high values, apart from the objective that controls voltage. In traditional radial distribution grids, line constraints are unimportant except for when planning the grid. Since all power is flowing downstream from the slack bus, then all lines have to be sufficiently sized to handle the peak potential power of all lines down stream. As such, a normal system has no way of optimizing line flow, apart from changing generation and load at each bus.

This, however, is not a traditional radial distribution grid. Power still flows downstream from the slack bus, but it may also flow upstream from the PV bus. As a consequence it is no longer possible to effortlessly assume that all lines have high enough capacity. For the base case of the system it is unlikely that there would be a major impact from including line constraints, but for the up-scaled PV scenario this is not the case. When the installed PV is at 5 MW, the transfer capacity of the lines to and from bus 30 could very well be a problem. This is a weakness in the model that should be accounted for in future versions.

Another aspect that affects not only the line constraints, but also other parts of the system, is the placement of the installed PV. Decentralizing PV generation will remove the strain on some lines, and would definitely not subject any line to more load than they would already be designed to handle. In fact if a new system were to be planned with decentralized PV, the line capacity of some of the lines closest to the tap changer could probably be decreased.

4.2.5 Modeling of supply by upstream grid

For every system where the total distributed generation is insufficient to cover all demand, it is important to have some way to model supply from the upstream grid. In this model the upstream grid contributes to voltage at slack bus via the tap changer, and power supply by injection into the slack bus. Solving the upstream grid like this is a good way to ensure that total demand in the distribution grid is covered, although once again this is mostly a "black box" approach. Modeling the upstream transmission system is, however, outside the scope of what this thesis intends to do.

Therefore, this modeling approach can be considered an acceptable simplification.

What could have been done differently is how the optimization is prioritized. As previously mentioned, the optimization problem had one single objective: Minimize voltage deviation from 1 P.U. As such, the optimization solver is not concerned with the cost of active and reactive power supplied by upstream grid. The impact of this single objective method can be seen clearly in the difference between figures 25 and 26.

This also means that in principle, the optimization solver is unconcerned with the losses attributed to how it handles the upstream supply. As such there is no real cost of loss either. In practice, however, the solver still tries to decrease line losses due to the voltage drop associated with them. Thus the solver has no concern for the cost of the power loss, but will still work to minimize it.

An additional shortcoming becomes clear when looking at figure 25: There is no real inertia in the system. As a consequence, the optimization problem will at any time find the amount of upstream supply that is ideal for this exact time increment, never basing the solution on how the supply was in the last one. While a distribution system could potentially only be a small part of a large transmission network, a couple of megawatts is not an insignificant load. Thus it would require some adjustment in the energy production, and most large generators are not turned on or off many times each day. While the lack of inertia can probably be ignored for a model with 1 hour time increments, it is an issue that would have to be alleviated in a model with smaller time increments.

4.2.6 Forecasting method

The method used for determining the chance constraints is, as mentioned, based on typical kurtosis of forecasting error from *H. Bludszuweit et al.*[22]. However, it is worth mentioning thatthis paper primarily focus on the forecasting error of wind, and not solar irradiation. Although there is a connection between wind and irradiation in a given day, there is some potential in improving the realism of the chance constraints by looking into a forecasting error PDF that is based on irradiation instead.

Furthermore, there is no assumption made regarding actual forecasting method. Forecasting is only covered when discussing the kurtosis of a typical day ahead forecast, but how the actual forecast is done remains outside the scope of this particular thesis.

It should also be noted that the model considers the same relative forecast error for all uncertain parameters. Thus the standard deviation is still different due to different equations for each uncertain parameter, but the relative maximum error is the same. This could potentially be changed, as the relative error of PV generation and demand are not necessarily the same, although related. In

future alterations of this work, it would be trivial to implement multiple forecasting errors

4.2.7 Real life value of an optimal solution

Although some of the parameters in this optimization problem are chance constrained, the result of the optimization is still deterministic. The solver knows all parameters and constraints for the whole day when doing the optimization, and thus the results are to the best of the solvers ability optimal. This is obviously not how a real distribution system functions.

Some aspects of the system, like how the inverter functions to supply reactive power, will always behave in the same way. Scheduling of the storage, however, is here optimized with the system knowing exactly what the future will look like. While it is advantageous to have a target SOC at the end of the day, the actual value at the end of the day will not be exactly the targeted value. As a consequence, scheduling batteries for voltage regulation the way it is done in the different scenarios of this model will not be as effective as shown in the results. Having good forecasts will, however, help to alleviate this.

5 Conclusion and future work

In this thesis, a voltage regulation model for distribution systems combining tap changer, photovoltaics and energy storage has been presented. The model focuses on minimizing the deviation of voltage in all buses of the distribution system. At the same time the uncertainty of demand and solar irradiation was taken into account, and this uncertainty was incorporated into the model using chance constraints. This uncertainty method has the big advantage that it is not dependent on historical data to be applicable.

The model was then implemented in the *Pyomo* optimization framework, and an optimal solution was found for the base case of the system. The model was then modified one part at a time, and the impact of the changes were further tested in *Pyomo* and discussed. Specific scenarios are tested, but the model is easily applicable to any distribution grid with photovoltaics.

The results reveal that there is a significant improvement in voltage profile if the tap changer is utilized together with distributed voltage regulators like PV and storage. Installation of distributed PV at one of the buses in the IEEE 33-bus test system, improved the voltage with an average of 0.0044 P.U for every bus at every time increment, while also reducing the deviation of the voltage peaks. Introducing a distributed PV + storage system drastically reduced the voltage peaks, and improved the average voltage with 0.012 P.U over all buses and time increments. Overall, the result of this analysis is that the voltage at the buses is significantly more affected by the placement of the voltage regulators rather than the size of the regulators.

Changing the value of the forecast error resulted in more narrow voltage constraints, and the base case PV-system failed to solve within a 90% certainty when the forecast error became 0.252. Increasing the scale of the distributed regulators was shown to improve this tolerance, and increasing the size of the inverter by 50% increased this tolerance to 0.757. Thus, the price of increased capacity can be viewed as the price of certainty.

Future work can be made by expanding the model to a larger network, as well as looking into the effect of installing PV at every bus. For a solution that is more true to real values it is also desirable to implement line constraints, as well as a more advanced model for energy storage.

Regarding uncertainty, the chance constrained model can be improved by looking into forecasting

error of solar irradiation rather than wind. Additionally, individual forecasting errors for different parameters can be implemented. It is also possible to expand the model by applying a different uncertainty model altogether. For instance, robust optimization is a more complex uncertainty modeling framework that can be applied.

Bibliography

[1] Denholm, P., O'Connell, M., Brinkman, G., & Jorgenson, J. 2015. Overgeneration from solar energy in california: A field guide to the duck chart. *National Renewable Energy Laboratory*. URL: https://www.nrel.gov/docs/fy16osti/65023.pdf.

[2] Zubi, G., Dufo-López, R., Carvalho, M., & Pasaoglu, G. jun 2018. The lithium-ion battery: State of the art and future perspectives. *Renewable and Sustainable Energy Reviews*, 89, 292–308. doi:10.1016/j.rser.2018.03.002.

[3] Masson, G. & Brunisholz, M. 2016 snapshot of global photovoltaic markets. Technical report, International Energy Agency, 2017. URL: http://www.iea-pvps.org/fileadmin/dam/public/report/statistics/IEA-PVPS_-_A_Snapshot_of_Global_PV_-_1992-2016__1_.pdf.

[4] Schmela, M., Masson, G., & Mai, N. N. T. Global market outlook for solar power. Technical report, SolarPower Europe, 2016. URL: http://www.solareb2b.it/wp-content/uploads/2016/06/SPE_GMO2016_full_version.pdf.

[5] Bird, L., Lew, D., Milligan, M., Carlini, E. M., Estanqueiro, A., Flynn, D., Gomez-Lazaro, E., Holttinen, H., Menemenlis, N., Orths, A., Eriksen, P. B., Smith, J. C., Soder, L., Sorensen, P., Altiparmakis, A., Yasuda, Y., & Miller, J. nov 2016. Wind and solar energy curtailment: A review of international experience. *Renewable and Sustainable Energy Reviews*, 65, 577–586. doi:10.1016/j.rser.2016.06.082.

[6] Yu, N. P., Sheng, H. Y., & Johnson, R. 2013. Economic valuation of wind curtailment rights. In *2013 IEEE Power & Energy Society General Meeting*. IEEE. doi:10.1109/pesmg.2013.6672796.

[7] Komarnicki, P., Lombardi, P., & Styczynski, Z. 2017. *Electric Energy Storage Systems*. Springer Berlin Heidelberg. doi:10.1007/978-3-662-53275-1.

[8] Doe global energy storage database. retrieved 08.11.2018. URL: http://www.energystorageexchange.org/projects/data_visualization.

[9] Bollen, M. H. J. & Sannino, A. jan 2005. Voltage control with inverter-based distributed generation. *IEEE Transactions on Power Delivery*, 20(1), 519–520. doi:10.1109/tpwrd.2004.834679.

[10] Hashemipour, N., Niknam, T., Aghaei, J., Farahmand, H., Korpas, M., Shafie-Khah, M., Osorio, G. J., & Catalao, J. P. S. jun 2018. A linear multi-objective operation model for smart distribution systems coordinating tap-changers, photovoltaics and battery energy storage. In *2018 Power Systems Computation Conference (PSCC)*. IEEE. doi:10.23919/pscc.2018.8442849.

[11] Collins, L. & Ward, J. sep 2015. Real and reactive power control of distributed PV inverters for overvoltage prevention and increased renewable generation hosting capacity. *Renewable Energy*, 81, 464–471. doi:10.1016/j.renene.2015.03.012.

[12] Demirok, E., González, P. C., Frederiksen, K. H. B., Sera, D., Rodriguez, P., & Teodorescu, R. oct 2011. Local reactive power control methods for overvoltage prevention of distributed solar inverters in low-voltage grids. *IEEE Journal of Photovoltaics*, 1(2), 174–182. doi:10.1109/jphotov.2011.2174821.

[13] Cagnano, A., Tuglie, E. D., Liserre, M., & Mastromauro, R. A. oct 2011. Online optimal reactive power control strategy of PV inverters. *IEEE Transactions on Industrial Electronics*, 58(10), 4549–4558. doi:10.1109/tie.2011.2116757.

[14] Festøy, M. H. Distributed voltage control in smart distribution systems. December 2018.

[15] Van ackooij, W. S. December 2013. Chance constrained programming : with applications in energy management. URL: http://tel.archives-ouvertes.fr/docs/00/97/85/19/PDF/thesis_van-ackooij.pdf.

[16] Hajian, M., Glavic, M., Rosehart, W. D., & Zareipour, H. August 2012. A chance-constrained optimization approach for control of transmission voltages. *IEEE Transactions on Power Systems*, 27(3), 1568–1576. doi:10.1109/tpwrs.2011.2181431.

[17] Kloppel, M., Gabash, A., Geletu, A., & Li, P. may 2013. Chance constrained optimal power flow with non-gaussian distributed uncertain wind power generation. In *2013 12th International Conference on Environment and Electrical Engineering*. IEEE. doi:10.1109/eeeic.2013.6549628.

[18] Geletu, A., Klöppel, M., Zhang, H., & Li, P. jul 2013. Advances and applications of chance-constrained approaches to systems optimisation under uncertainty. *International Journal of Systems Science*, 44(7), 1209–1232. doi:10.1080/00207721.2012.670310.

[19] Yang, N. & Wen, F. aug 2005. A chance constrained programming approach to transmission system expansion planning. *Electric Power Systems Research*, 75(2-3), 171–177. doi:10.1016/j.epsr.2005.02.002.

[20] Fan, M., Vittal, V., Heydt, G. T., & Ayyanar, R. may 2013. Probabilistic power flow analysis with generation dispatch including photovoltaic resources. *IEEE Transactions on Power Systems*, 28(2), 1797–1805. doi:10.1109/tpwrs.2012.2219886.

[21] Akhavan-Hejazi, H. & Mohsenian-Rad, H. May 2018. Energy storage planning in active distribution grids: A chance-constrained optimization with non-parametric probability functions. *IEEE Transactions on Smart Grid*, 9(3), 1972–1985. doi:10.1109/TSG.2016.2604286.

[22] Bludszuweit, H., Dominguez-Navarro, J., & Llombart, A. August 2008. Statistical analysis of wind power forecast error. *IEEE Transactions on Power Systems*, 23(3), 983–991. doi:10.1109/tpwrs.2008.922526.

[23] Stott, B. & Hobson, E. sep 1978. Power system security control calculations using linear programming, part i. *IEEE Transactions on Power Apparatus and Systems*, PAS-97(5), 1713–1720. doi:10.1109/tpas.1978.354664.

[24] Shchetinin, D., Rubira, T. T. D., & Hug-Glanzmann, G. October 2018. On the construction of linear approximations of line flow constraints for ac optimal power flow. *IEEE Transactions on Power Systems*. doi:10.1109/TPWRS.2018.2874173.

[25] Garces, A. jan 2016. A linear three-phase load flow for power distribution systems. *IEEE Transactions on Power Systems*, 31(1), 827–828. doi:10.1109/tpwrs.2015.2394296.

[26] Dall'Anese, E., Baker, K., & Summers, T. September 2017. Chance-constrained ac optimal power flow for distribution systems with renewables. *IEEE Transactions on Power Systems*, 32(5), 3427–3438. doi:10.1109/TPWRS.2017.2656080.

[27] Dhople, S. V., Guggilam, S. S., & Chen, Y. C. 2015. Linear approximations to ac power flow in rectangular coordinates.

[28] Hashemipour, S. N. & Aghaei, J. December 2017. Chance constrained power-flow for voltage regulation in distribution systems. In *2017 Smart Grid Conference (SGC)*, 1–6. doi:10.1109/SGC.2017.8308848.

[29] Chandy, K. M., Low, S. H., Topcu, U., & Xu, H. dec 2010. A simple optimal power flow model with energy storage. In *49th IEEE Conference on Decision and Control (CDC)*. IEEE. doi:10.1109/cdc.2010.5718193.

[30] Hart, W. E., Laird, C., Watson, J.-P., & Woodruff, D. L. 2012. *Pyomo – Optimization Modeling in Python*. Springer US. doi:10.1007/978-1-4614-3226-5.

A Appendix: Simulation data

Table 4: 24 hour load and irradiation data.

Hour	Load	Solar irradiation
1	0.6000	0
2	0.5667	0
3	0.4333	0
4	0.3667	0
5	0.3000	0
6	0.3000	0
7	0.3333	0
8	0.4000	0
9	0.4667	0.1899
10	0.5667	0.5225
11	0.6000	0.5699
12	0.6333	0.9499
13	0.7000	0.7599
14	0.7333	0.7409
15	0.7333	0.6966
16	0.7333	0.0189
17	0.8000	0
18	0.8333	0
19	0.9000	0
20	1.0000	0
21	0.9667	0
22	0.8667	0
23	0.7333	0
24	0.6667	0

B Appendix: Summary of system data

Table 5: Summary of system data for different optimization scenarios.

System	Normal grid	Base case PV	PV + storage	5·PV + storage	Decentralized PV + storage
Base voltage[V]	12660	12660	12660	12660	12660
PV buses	n/a	30	30	30	14, 21, 24, 30
PV installed at PV buses[MW]	n/a	1	1	5	1
Inverter size at PV buses[MVA]	n/a	1.054	1.054	5.27	1.054
Storage power at PV buses[MW]	n/a	n/a	5	5	3
Storage capacity at PV buses[MWh]	n/a	n/a	15	30	9

C Appendix: Supporting figures

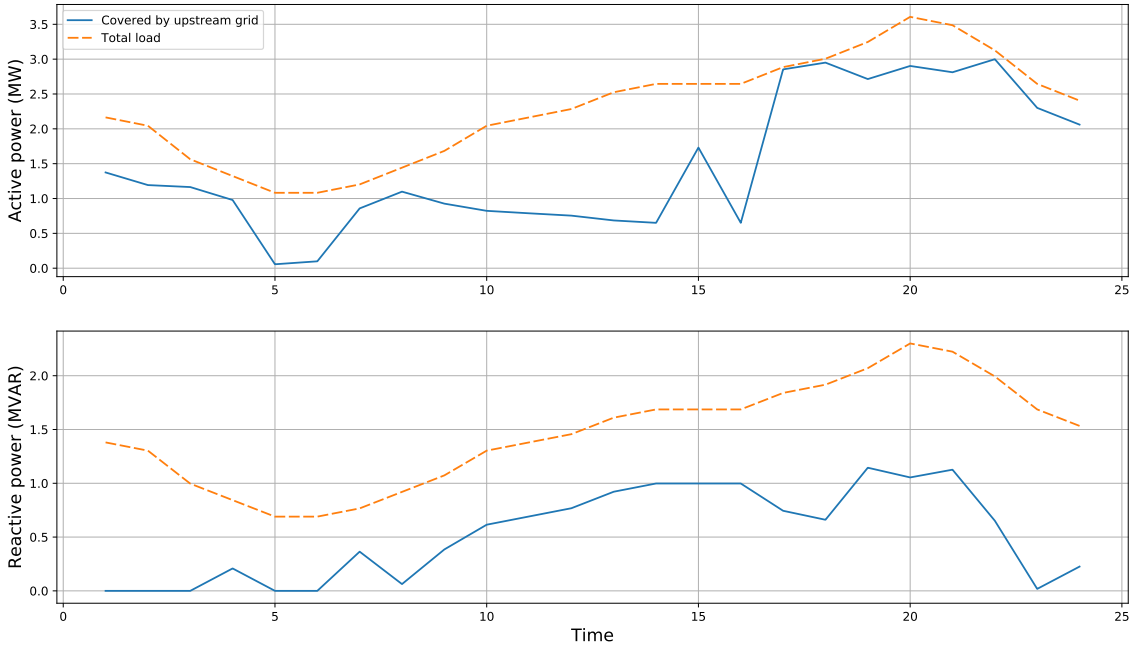

Figure 33: Power covered by upstream grid for each hour of the day, decentralized case.